CHAPTER

9

BROADBAND DIPOLES AND MATCHING TECHNIQUES

9.1 INTRODUCTION

In Chapter 4 the radiation properties (pattern, directivity, input impedance, mutual impedance, etc.) of very thin wire antennas were investigated by assuming that the current distribution, which in most cases is sinusoidal, is known. In practice, infinitely thin (electrically) wires are not realizable but can be approximated. In addition, their radiation characteristics (such as pattern, impedance, gain, etc.) are very sensitive to frequency. The degree to which they change as a function of frequency depends on the antenna bandwidth. For applications that require coverage of a broad range of frequencies, such as television reception of all channels, wide-band antennas are needed. There are numerous antenna configurations, especially of arrays, that can be used to produce wide bandwidths. Some simple and inexpensive dipole configurations, including the conical and cylindrical dipoles, can be used to accomplish this to some degree.

For a finite diameter wire (usually $d > 0.05\lambda$) the current distribution may not be sinusoidal and its effect on the radiation pattern of the antenna is usually negligible. However, it has been shown that the current distribution has a pronounced effect on the input impedance of the wire antenna, especially when its length is such that a near null in current occurs at its input terminals. The effects are much less severe when a near current maximum occurs at the input terminals.

Historically there have been three methods that were used to take into account the finite conductor thickness. The first method treats the problem as boundary-value problem [1], the second as a tapered transmission line or electromagnetic horn [2], and the third finds the current distribution on the wire from an integral equation [3]. The boundary-value approach is well suited for idealistic symmetrical geometries (e.g., ellipsoids, prolate spheroids) which cannot be used effectively to approximate more practical geometries such as the cylinder. The method expresses the fields in terms of an infinite series of free oscillations or natural modes whose coefficients are chosen to satisfy the conditions of the driving source. For the assumed idealized configurations, the method does lead to very reliable data, but it is very difficult to know how to approximate more practical geometries (such as a cylinder) by the more

441

idealized configurations (such as the prolate spheroid). For these reasons the boundary-value method is not very practical and will not be pursued any further in this text.

In the second method Schelkunoff represents the antenna as a two-wire uniformly tapered transmission line, each wire of conical geometry, to form a biconical antenna. Its solution is obtained by applying transmission line theory (incident and reflected waves), so well known to the average engineer. The analysis begins by first finding the radiated fields which in turn are used, in conjunction with transmission line theory, to find the input impedance.

For the third technique, the main objectives are to find the current distribution on the antenna and in turn the input impedance. These were accomplished by Hallén by deriving an integral equation for the current distribution whose approximate solution, of different orders, was obtained by iteration and application of boundary conditions. Once a solution for the current is formed, the input impedance is determined by knowing the applied voltage at the feed terminals.

The details of the second method will follow in summary form. The integral equation technique of Hallén, along with that of Pocklington, form the basis of Moment Method techniques which were discussed in Chapter 8.

9.2   BICONICAL ANTENNA

One simple configuration that can be used to achieve broadband characteristics is the biconical antenna formed by placing two cones of infinite extent together, as shown in Figure 9.1(a). This can be thought to represent a uniformly tapered transmission line. The application of a voltage V_i at the input terminals will produce outgoing spherical waves, as shown in Figure 9.1(b), which in turn produce at any point $(r, \theta = \theta_c, \phi)$ a current I along the surface of the cone and voltage V between the cones (Figure 9.2). These can then be used to find the characteristic impedance of the transmission line, which is also equal to the input impedance of an infinite geometry. Modifications to this expression, to take into account the finite lengths of the cones, will be made using transmission line analogy.

9.2.1 Radiated Fields

The analysis begins by first finding the radiated E- and H-fields between the cones, assuming dominant TEM mode excitation (E and H are transverse to the direction of propagation). Once these are determined for any point (r, θ, ϕ), the voltage V and current I at any point on the surface of the cone $(r, \theta = \theta_c, \phi)$ will be formed. From Faraday's law we can write that
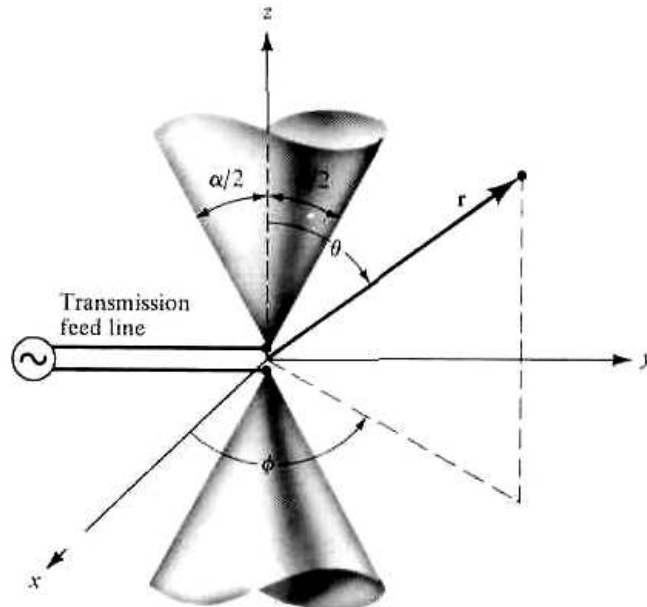
$$\nabla \times \mathbf{E} = -j\omega\mu\mathbf{H} \tag{9-1}$$

which when expanded in spherical coordinates and assuming that the E-field has only an E_θ component independent of ϕ, reduces to
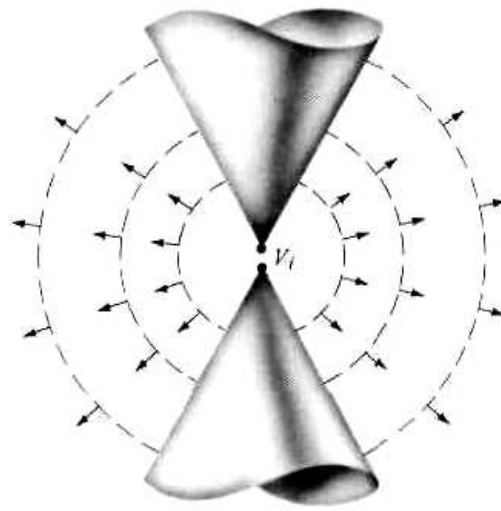
$$\nabla \times \mathbf{E} = \hat{a}_\phi \frac{1}{r} \frac{\partial}{\partial r} (rE_\theta) = -j\omega\mu(\hat{a}_r H_r + \hat{a}_\theta H_\theta + \hat{a}_\phi H_\phi) \tag{9-2}$$

Since H only has an H_ϕ component, necessary to form the TEM mode with E_θ, (9-2) can be written as

$$\frac{1}{r} \frac{\partial}{\partial r} (rE_\theta) = -j\omega\mu H_\phi \tag{9-2a}$$

(a) Biconical geometry

(b) Spherical waves

Figure 9.1   Biconical antenna geometry and radiated spherical waves.

From Ampere's law we have that

$$\nabla \times \mathbf{H} = +j\omega\epsilon\mathbf{E} \tag{9-3}$$

which when expanded in spherical coordinates, and assuming only E_θ and H_ϕ components independent of ϕ, reduces to

$$\hat{\mathbf{a}}_r \frac{1}{r^2 \sin\theta} \left[\frac{\partial}{\partial\theta} (r \sin\theta H_\phi) \right] - \hat{\mathbf{a}}_\theta \frac{1}{r \sin\theta} \left[\frac{\partial}{\partial r} (r \sin\theta H_\phi) \right] = +j\omega\epsilon(\hat{\mathbf{a}}_\theta E_\theta) \tag{9-4}$$

which can also be written as

$$\frac{\partial}{\partial\theta} (r \sin\theta H_\phi) = 0 \tag{9-4a}$$

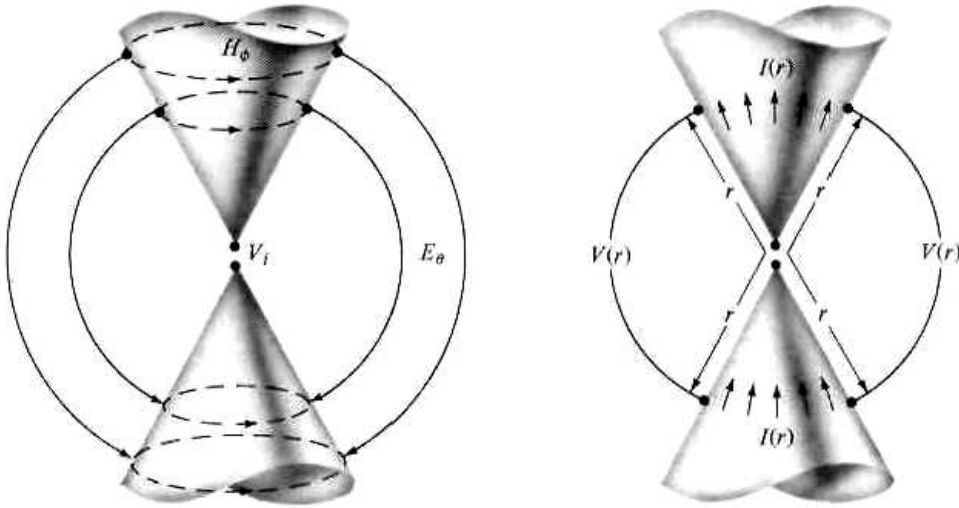$$\frac{1}{r \sin\theta} \frac{\partial}{\partial r} (r \sin\theta H_\phi) = -j\omega\epsilon E_\theta \tag{9-4b}$$

Figure 9.2 Electric and magnetic fields, and associated voltages and currents, for a biconical antenna.

Rewriting (9-4b) as

$$\frac{1}{r}\frac{\partial}{\partial r}(rH_\phi) = -j\omega\epsilon E_\theta \tag{9-5}$$

and substituting it into (9-2a) we form a differential equation for H_ϕ as

$$-\frac{1}{j\omega\epsilon r}\frac{\partial}{\partial r}\left[\frac{\partial}{\partial r}(rH_\phi)\right] = -j\omega\mu H_\phi \tag{9-6}$$

or

$$\frac{\partial^2}{\partial r^2}(rH_\phi) = -\omega^2\mu\epsilon(rH_\phi) = -k^2(rH_\phi) \tag{9-6a}$$

A solution for (9-6a) must be obtained to satisfy (9-4a). To meet the condition of (9-4a), the θ variations of H_ϕ must be of the form

$$H_\phi = \frac{f(r)}{\sin\theta} \tag{9-7}$$

A solution of (9-6a), which also meets the requirements of (9-7) and represents an outward traveling wave, is

$$H_\phi = \frac{H_0}{\sin\theta}\frac{e^{-jkr}}{r} \tag{9-8}$$

where

$$f(r) = H_0\frac{e^{-jkr}}{r} \tag{9-8a}$$

An inward traveling wave is also a solution but does not apply to the infinitely long structure.

Since the field is of TEM mode, the electric field is related to the magnetic field by the intrinsic impedance, and we can write it as

$$E_\theta = \eta H_\phi = \eta \frac{H_0}{\sin \theta} \frac{e^{-jkr}}{r} \tag{9-9}$$

In Figure 9.2(a) we have sketched the electric and magnetic field lines in the space between the two conical structures. The voltage produced between two corresponding points on the cones, a distance r from the origin, is found by

$$V(r) = \int_{\alpha/2}^{\pi-\alpha/2} \mathbf{E} \cdot d\mathbf{l} = \int_{\alpha/2}^{\pi-\alpha/2} (\hat{\mathbf{a}}_\theta E_\theta) \cdot (\hat{\mathbf{a}}_\theta r d\theta) = \int_{\alpha/2}^{\pi-\alpha/2} E_\theta r d\theta \tag{9-10}$$

or by using (9-9)

$$V(r) = \eta H_0 e^{-jkr} \int_{\alpha/2}^{\pi-\alpha/2} \frac{d\theta}{\sin \theta} = \eta H_0 e^{-jkr} \ln\left[\frac{\cot(\alpha/4)}{\tan(\alpha/4)}\right]$$

$$V(r) = 2\eta H_0 e^{-jkr} \ln\left[\cot\left(\frac{\alpha}{4}\right)\right] \tag{9-10a}$$

The current on the surface of the cones, a distance r from the origin, is found by using (9-8) as

$$I(r) = \int_0^{2\pi} H_\phi r \sin \theta \, d\phi = H_0 e^{-jkr} \int_0^{2\pi} d\phi = 2\pi H_0 e^{-jkr} \tag{9-11}$$

In Figure 9.2(b) we have sketched the voltage and current at a distance r from the origin.

9.2.2 Input Impedance

A. Infinite Cones

Using the voltage of (9-10a) and the current of (9-11), we can write the characteristic impedance as

$$Z_c = \frac{V(r)}{I(r)} = \frac{\eta}{\pi} \ln\left[\cot\left(\frac{\alpha}{4}\right)\right] \tag{9-12}$$

Since the characteristic impedance is not a function of the radial distance r, it also represents the input impedance at the antenna feed terminals of the infinite structure. For a free-space medium, (9-12) reduces to

$$\boxed{Z_c = Z_{in} = 120 \ln\left[\cot\left(\frac{\alpha}{4}\right)\right]} \tag{9-12a}$$

which is a pure resistance. For small cone angles

$$Z_{in} = \frac{\eta}{\pi} \ln\left[\cot\left(\frac{\alpha}{4}\right)\right] = \frac{\eta}{\pi} \ln\left[\frac{1}{\tan(\alpha/4)}\right] \simeq \frac{\eta}{\pi} \ln\left(\frac{4}{\alpha}\right) \tag{9-12b}$$

Variations of Z_{in} as a function of the half-cone angle $\alpha/2$ are shown plotted in Figure 9.3(a) for $0° < \alpha/2 \leq 90°$ and in Figure 9.3(b) in an expanded scale for
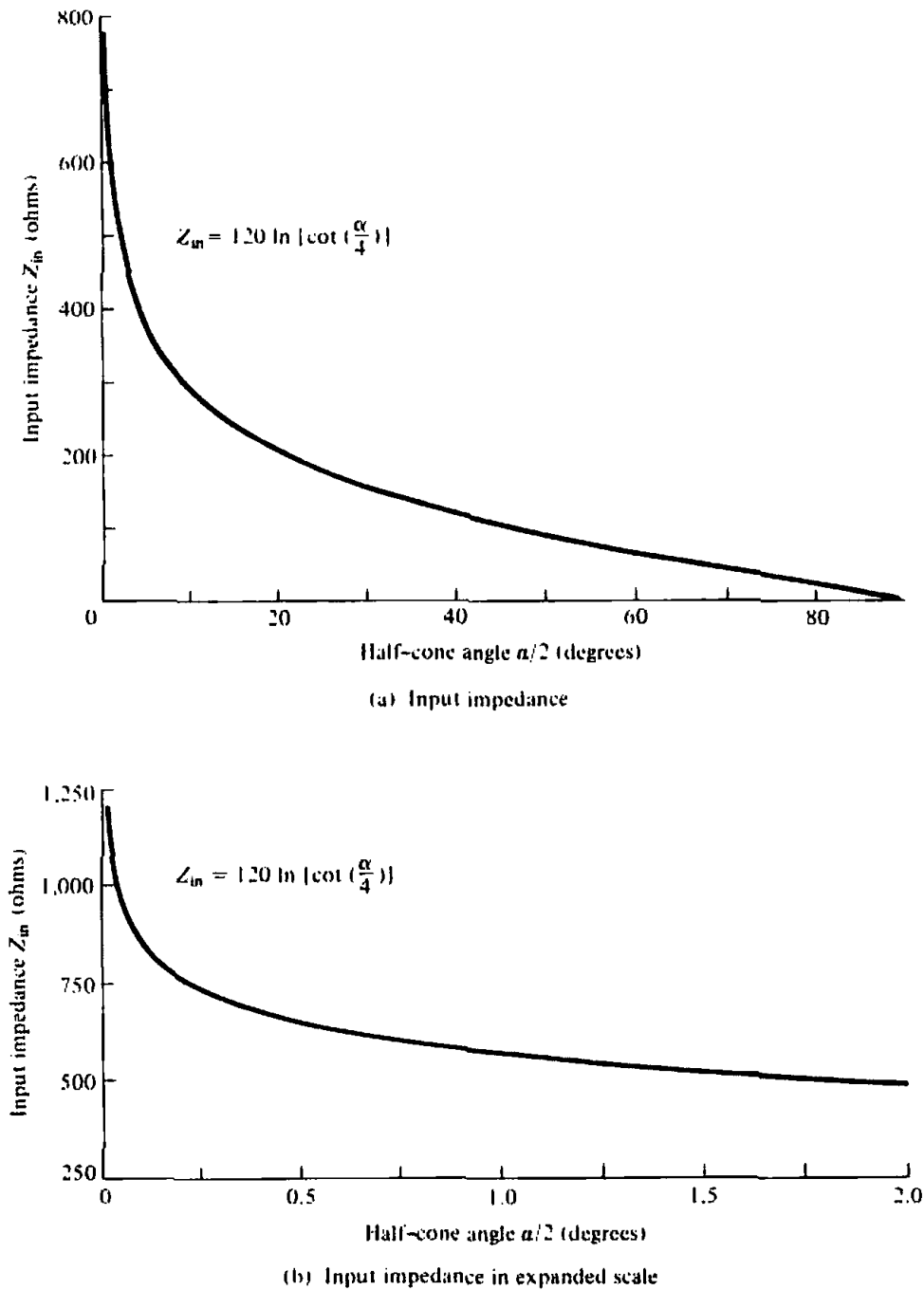
$Z_{in} = 120 \ln |\cot(\frac{\alpha}{4})|$

(a) Input impedance

$Z_{in} = 120 \ln |\cot(\frac{\alpha}{4})|$

(b) Input impedance in expanded scale

Figure 9.3   Input impedance of an infinitely long biconical antenna radiating in free-space.

$0° < \alpha/2 \leq 2°$. Although the half-cone angle is not very critical in the design, it is usually chosen so that the characteristic impedance of the biconical configuration is nearly the same as that of the transmission line to which it will be attached. Small angle biconical antennas are not very practical but wide-angle configurations ($30° < \alpha/2 < 60°$) are frequently used as broadband antennas.

The radiation resistance of (9-12) can also be obtained by first finding the total radiated power

$$ P_{rad} = \oint_S \mathbf{W}_{av} \cdot d\mathbf{s} = \int_0^{2\pi} \int_{\alpha/2}^{\pi-\alpha/2} \frac{|E|^2}{2\eta} r^2 \sin\theta \, d\theta \, d\phi = \pi\eta|H_0|^2 \int_0^{\pi-\alpha/2} \frac{d\theta}{\sin\theta} $$

$$P_{rad} = 2\pi\eta|H_0|^2 \ln\left[\cot\left(\frac{\alpha}{4}\right)\right]$$ (9-13)

and by using (9-11) evaluated at $r = 0$ we form

$$R_r = \frac{2P_{rad}}{[I(0)]^2} = \frac{\eta}{\pi}\ln\left[\cot\left(\frac{\alpha}{4}\right)\right]$$ (9-14)

which is identical to (9-12).

B. Finite Cones

The input impedance of (9-12) or (9-14) is for an infinitely long structure. To take into account the finite dimensions in determining the input impedance, Schelkunoff [2] has devised an ingenious method where he assumes that for a finite length cone $(r = l/2)$ some of the energy along the surface of the cone is reflected while the remaining is radiated. Near the equator most of the energy is radiated. This can be viewed as a load impedance connected across the ends of the cones. The electrical equivalent is a transmission line of characteristic impedance Z_c terminated in a load impedance Z_L. Computed values [4] for the input resistance and reactance of small angle cones are shown in Figure 9.4. It is apparent that the antenna becomes more broadband (its resistance and reactance variations are less severe) as the cone angle increases.

The biconical antenna represents one of the canonical problems in antenna theory, and its model is well suited for examining general characteristics of dipole-type antennas.

C. Unipole

Whenever one of the cones is mounted on an infinite plane conductor (i.e., the lower cone is replaced by a ground plane), it forms a unipole and its input impedance is one-half of the two-cone structure. Input impedances for unipoles of various cone angles as a function of the antenna length l have been measured [5]. Radiation patterns of biconical dipoles fed by coaxial lines have been computed by Papas and King [6].

9.3 TRIANGULAR SHEET, BOW-TIE, AND WIRE SIMULATION

Because of their broadband characteristics, biconical antennas have been employed for many years in the VHF and UHF frequency ranges. However, the solid or shell biconial structure is so massive for most frequencies of operation that it is impractical to use. Because of its attractive radiation characteristics, compared to those of other single antennas, realistic variations to its mechanical structure have been sought while retaining as much of the desired electrical features as possible.

Geometrical approximations to the solid or shell conical unipole or biconical antenna are the triangular sheet and bow-tie antennas shown in Figures 9.5(a) and (b), respectively, each fabricated from sheet metal. The triangular sheet has been investigated experimentally by Brown and Woodward [5]. Each of these antennas can also be simulated by a wire along the periphery of its surface which reduces significantly the weight and wind resistance of the structure. The computed input impedances and radiation patterns of wire bow-tie antennas, when mounted above a ground plane,
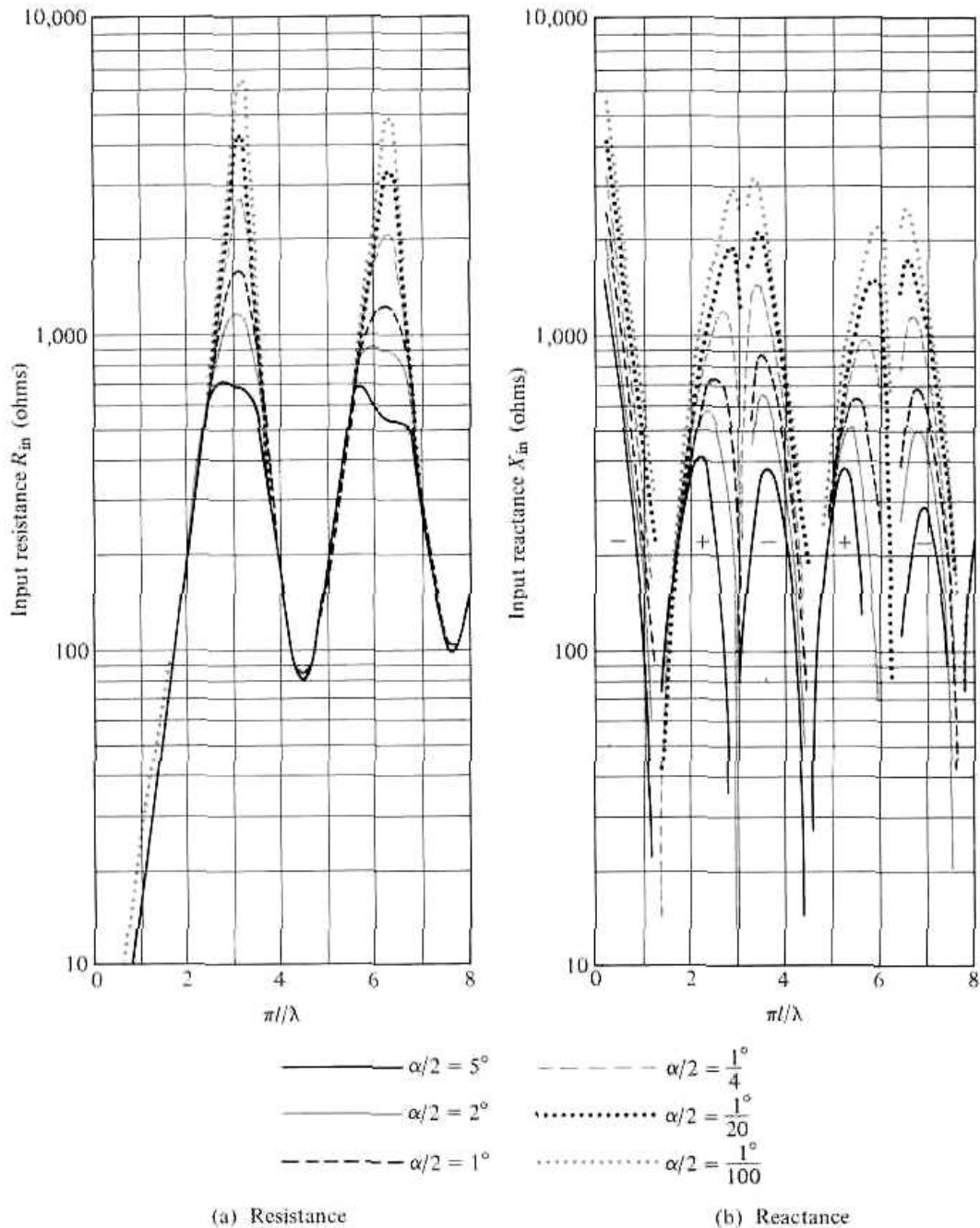
(a) Resistance

(b) Reactance

Figure 9.4 Input impedance (at feed terminals) of finite length biconical antenna. (SOURCE: H. Jasik (ed.), *Antenna Engineering Handbook*, McGraw-Hill, New York, 1961, Chapter 3)

have been computed using the Moment Method [7]. The impedance is shown plotted in Figure 9.6. A comparison of the results of Figure 9.6 with those of reference [5] reveals that the bow-tie antenna does not exhibit as broadband characteristics (i.e., nearly constant resistance and essentially zero reactance over a large frequency range) as the corresponding solid biconical antenna for $30° < \alpha < 90°$. Also for a given flare angle the resistance and reactance of the bow-tie wire structure fluctuate more than for a triangular sheet antenna. Thus the wire bow-tie is very narrowband as compared to the biconical surface of revolution or triangular sheet antenna.

In order to simulate better the attractive surface of revolution of a biconical antenna by low-mass structures, multielement intersecting wire bow-ties were employed as shown in Figure 9.5(c). It has been shown that eight or more intersecting
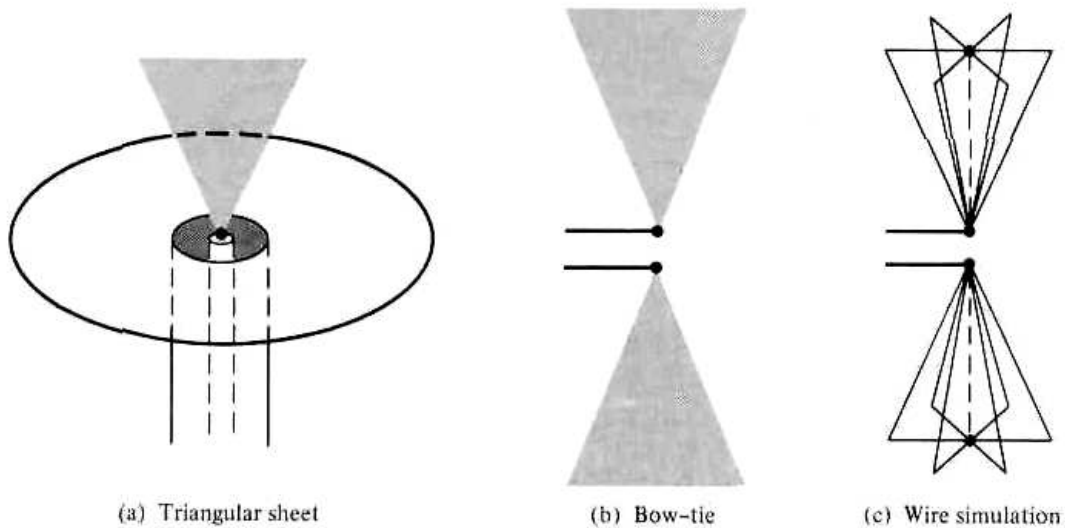
(a) Triangular sheet   (b) Bow-tie   (c) Wire simulation

Figure 9.5 Triangular sheet, bow-tie, and wire simulation of biconical antenna.

wire-constructed bow-ties can approximate reasonably well the radiation characteristics of a conical body-of-revolution antenna.

9.4 CYLINDRICAL DIPOLE

Another simple and inexpensive antenna whose radiation characteristics are frequency dependent is a cylindrical dipole (i.e., a wire of finite diameter and length) of the form shown in Figure 9.7. Thick dipoles are considered broadband while thin dipoles are more narrowband. This geometry can be considered to be a special form of the biconical antenna when $\alpha = 0°$. A thorough analysis of the current, impedance, pattern, and other radiation characteristics can be performed using the Moment Method. With that technique the antenna is analyzed in terms of integral formulations of the Hallén and Pocklington type which can be evaluated quite efficiently by the Moment Method. The analytical formulation of the Moment Method has been presented in Chapter 8. In this section we want to present, in summary form, some of its performance characteristics.

9.4.1 Bandwidth

As has been pointed out previously, a very thin linear dipole has very narrowband input impedance characteristics. Any small perturbations in the operating frequency will result in large changes in its operational behavior. One method by which its acceptable operational bandwidth can be enlarged will be to decrease the l/d ratio. For a given antenna, this can be accomplished by holding the length the same and increasing the diameter of the wire. For example, an antenna with a $l/d \simeq 5,000$ has an acceptable bandwidth of about 3%, which is a small fraction of the center frequency. An antenna of the same length but with a $l/d \simeq 260$ has a bandwidth of about 30%.

9.4.2 Input Impedance

The input impedance (resistance and reactance) of a very thin dipole of length l and diameter d can be computed using (8-60a)–(8-61b). As the radius of the wire increases,
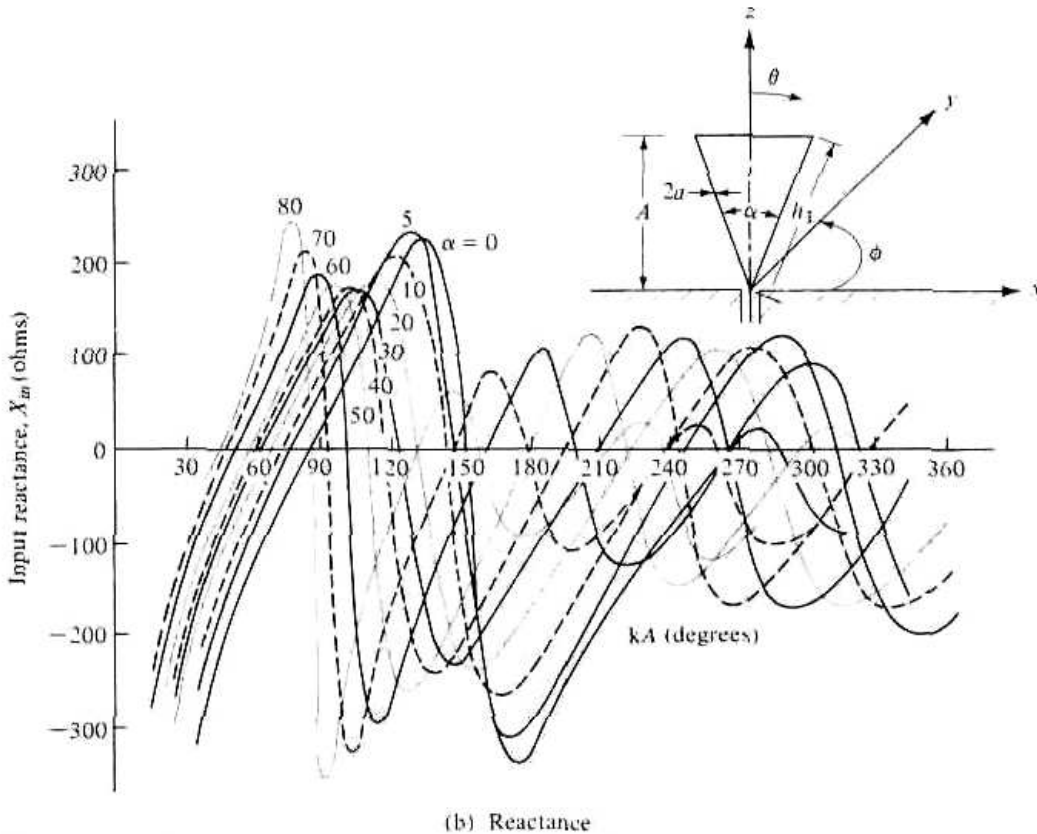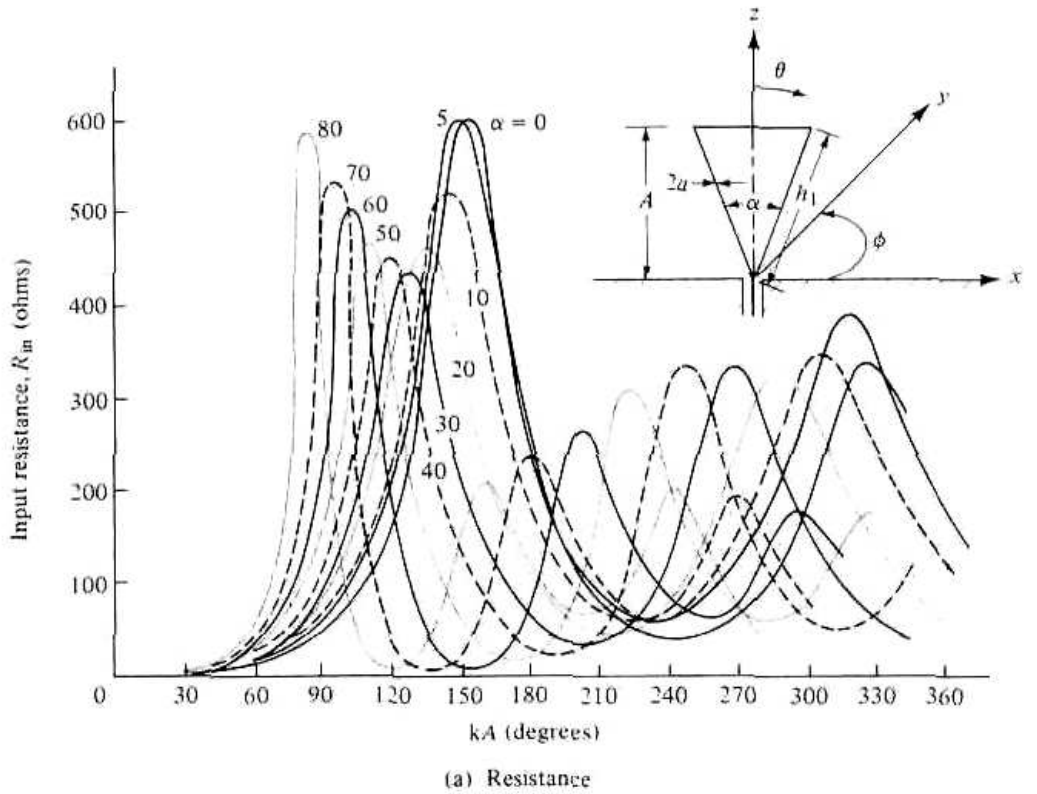
(a) Resistance

(b) Reactance

Figure 9.6 Computed impedance of wire bow-tie (or wire unipole) as a function of length for various included angles. (SOURCE: C. E. Smith, C. M. Butler, and K. R. Umashankar, "Characteristics of Wire Biconical Antenna," *Microwave Journal,* pp. 37–40, September 1979)
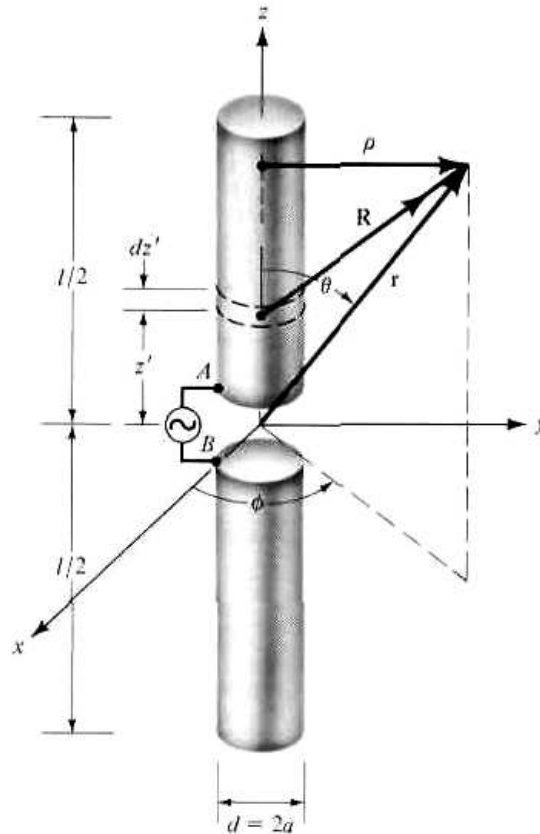
Figure 9.7 Center-fed cylindrical antenna configuration.

these equations become inaccurate. However, using integral equation analyses such as the Moment Method of Chapter 8, input impedances can be computed for wires with different l/d ratios. In general, it has been observed that for a given length wire its impedance variations become less sensitive as a function of frequency as the l/d ratio decreases. Thus more broadband characteristics can be obtained by increasing the diameter of a given wire. To demonstrate this, in Figures 9.8(a) and (b) we have plotted, as a function of length, the input resistance and reactance of dipoles with $l/d = 10^4 (\Omega = 19.81)$, $50(\Omega = 9.21)$, and $25(\Omega = 6.44)$ where $\Omega = 2 \ln(2l/d)$. For $l/d = 10^4$ the values were computed using (8-60a) and (8-61a) and then transferred to the input terminals by (8-60b) and (8-61b), respectively. The others were computed using the Moment Method techniques of Chapter 8. It is noted that the variations of each are less pronounced as the l/d ratio decreases, thus providing greater bandwidth.
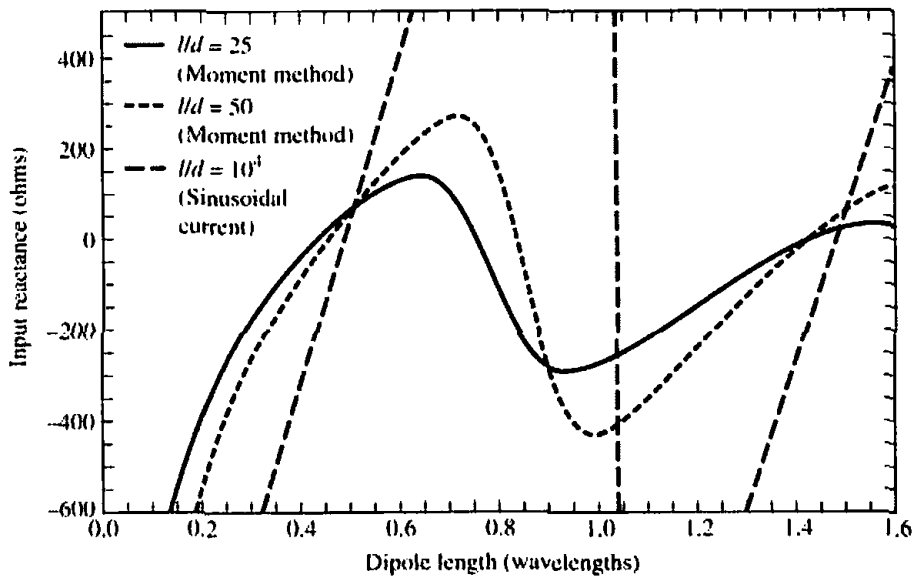
Measured input resistances and reactances for a wide range of constant l/d ratios have been reported [8]. These curves are for a cylindrical antenna driven by a coaxial cable mounted on a large ground plane on the earth's surface. Thus they represent half of the input impedance of a center-fed cylindrical dipole radiating in free-space. The variations of the antenna's electrical length were obtained by varying the frequency while the length-to-diameter (l/d) ratio was held constant.

9.4.3. Resonance and Ground Plane Simulation

The imaginary part of the input impedance of a linear dipole can be eliminated by making the total length, l, of the wire slightly less than an integral number of half-wavelengths (i.e., l slight less than $n\lambda/2$, $n = 1, 2, 3, 4, \ldots$). The amount of reduction in length, is a function of the radius of the wire, and it can be determined for thin
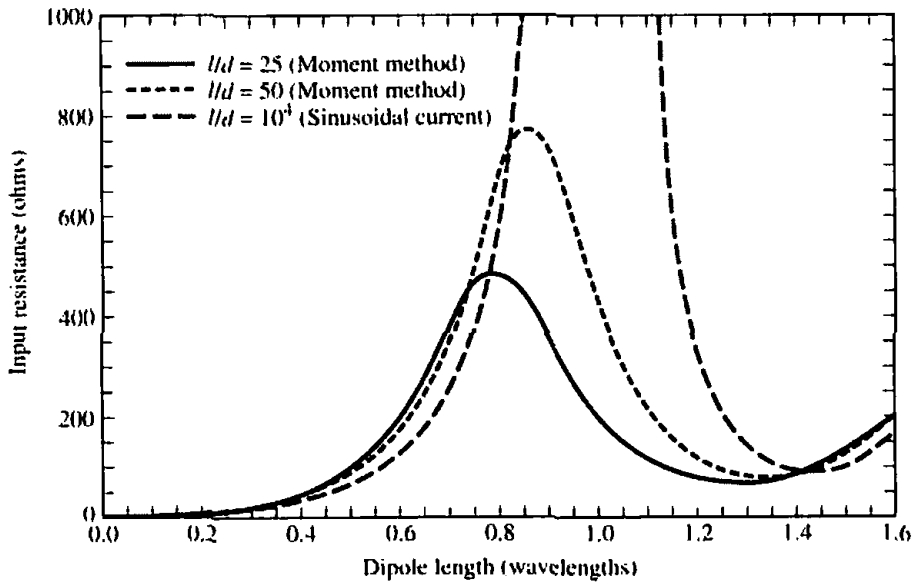
(a) Input resistance

(b) Input reactance

Figure 9.8 (a) Input resistance and reactance of wire dipoles.

wires iteratively using (8-60b) and (8-61b). At the resonance length, the resistance can then be determined using (8-60a) and (8-61a). Empirical equations for approximating the length, impedance, and the order of resonance of the cylindrical dipoles are found in Table 9.1 [9]. R_n is called the natural resistance and represents the geometric mean resistance at an odd resonance and at the next higher even resonance. For a cylindrical stub above a ground plane, as shown in Figure 9.9, the corresponding values are listed in Table 9.2 [9].

To reduce the wind resistance, to simplify the design, and to minimize the costs, a ground plane is often simulated, especially at low frequencies, by crossed wires as shown in Figure 9.9(b). Usually only two crossed wires (four radials) are employed. A larger number of radials results in a better simulation of the ground plane. Ground planes are also simulated by wire mesh. The spacing between the wires is usually

Table 9.1 CYLINDRICAL DIPOLE RESONANCES

	First Resonance	Second Resonance	Third Resonance	Fourth Resonance
LENGTH	$0.48\lambda F$	$0.96\lambda F$	$1.44\lambda F$	$1.92\lambda F$
RESISTANCE (ohms)	67	$\dfrac{R_n^2}{67}$	95	$\dfrac{R_n^2}{95}$

$$F = \frac{l/2a}{1 + l/2a} \ ; \ R_n = 150 \ \log_{10}(l/2a)$$

selected to be equal or smaller than $\lambda/10$. The flat or shaped reflecting surfaces for UHF educational TV are usually realized approximately by using wire mesh.

9.4.4 Radiation Patterns

The theory for the patterns of infinitesimally thin wires was developed in Chapter 4. Although accurate patterns for finite diameter wires can be computed using current distributions obtained by the Moment Method of Chapter 8, the patterns calculated using ideal sinusoidal current distributions, valid for infinitely small diameters, provide a good first-order approximation even for relatively thick cylinders. To illustrate this, in Figure 9.10 we have plotted the relative patterns for $l = 3\lambda/2$ with $l/d = 10^4 (\Omega = 19.81)$, $50(\Omega = 9.21)$, $25(\Omega = 6.44)$, and $8.7(\Omega = 5.71)$, where $\Omega = 2 \ln(2l/d)$. For $l/d = 10^4$ the current distribution was assumed to be purely sinusoidal, as given by (4-56); for the others, the Moment Method techniques of Chapter 8 were used. The patterns were computed using the Moment Method formulations outlined in Section 8.4. It is noted that the pattern is essentially unaffected by the thickness of the wire in regions of intense radiation. However, as the radius of the wire increases, the minor lobes diminish in intensity and the nulls are replaced by low-level radiation. The same characteristics have been observed for other length dipoles such as $l = \lambda/2$, λ and 2λ. The input impedance for the $l = \lambda/2$ and $l = 3\lambda/2$ dipoles, with $l/d = 10^4$, 50, and 25, is equal to

$l = \lambda/2$	$l = 3\lambda/2$	
$Z_{in}(l/d = 10^4) = 73 + j42.5$	$Z_{in}(l/d = 10^4) = 105.49 + j45.54$	
$Z_{in}(l/d = 50) = 85.8 + j54.9$	$Z_{in}(l/d = 50) = 103.3 + j9.2$	(9-15)
$Z_{in}(l/d = 25) = 88.4 + j27.5$	$Z_{in}(l/d = 25) = 106.8 + j4.9$	

Table 9.2 CYLINDRICAL STUB RESONANCES

	First Resonance	Second Resonance	Third Resonance	Fourth Resonance
LENGTH	$0.24\lambda F'$	$0.48\lambda F'$	$0.72\lambda F'$	$0.96\lambda F'$
RESISTANCE (ohms)	34	$\dfrac{(R_n')^2}{34}$	48	$\dfrac{(R_n')^2}{48}$

$$F' = \frac{l/a}{1 + l/a} \ ; \ R_n' = 75 \ \log_{10}(l/a)$$

(a) Cylindrical monopole
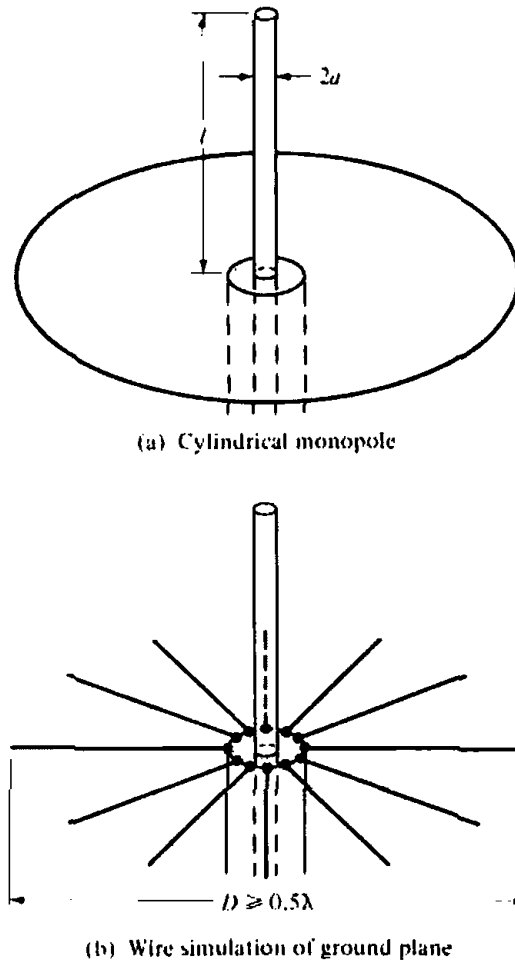
(b) Wire simulation of ground plane

Figure 9.9 Cylindrical monopole above circular solid and wire-simulated ground planes.

9.4.5 Equivalent Radii

Up to now, the formulations for the current distribution and the input impedance assume that the cross section of the wire is constant and of radius a. An electrical equivalent radius can be obtained for some uniform wires of noncircular cross section. This is demonstrated in Table 9.3 where the actual cross sections and their equivalent radii are illustrated.

The equivalent radius concept can be used to obtain the antenna or scattering characteristics of electrically small wires of arbitrary cross sections. It is accomplished by replacing the noncircular cross section wire with a circular wire whose radius is the "equivalent" radius of the noncircular cross section. In electrostatics, the equivalent radius represents the radius of a circular wire whose capacitance is equal to that of the noncircular geometry. This definition can be used at all frequencies provided the wire remains electrically small. The circle with equivalent radius lies between the circles which circumscribe and inscribe the geometry and which together bound the noncircular cross section.

9.4.6 Dielectric Coating

Up to now it has been assumed that the wire antennas are radiating into free-space. The radiation characteristics of a wire antenna (current distribution, far-field pattern,
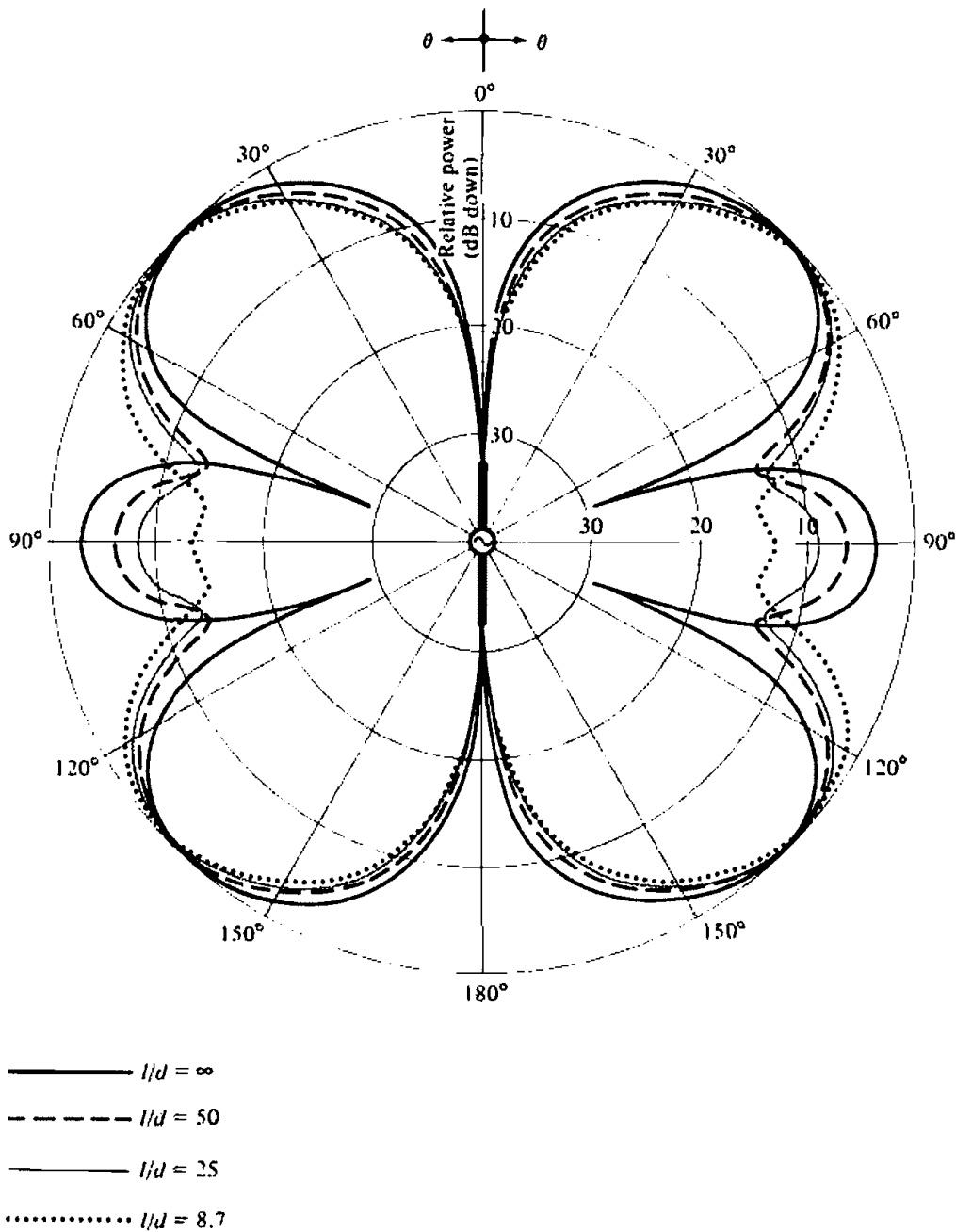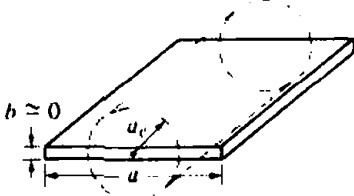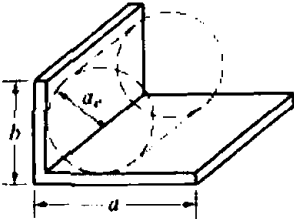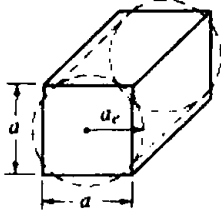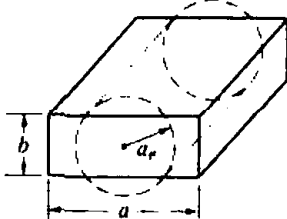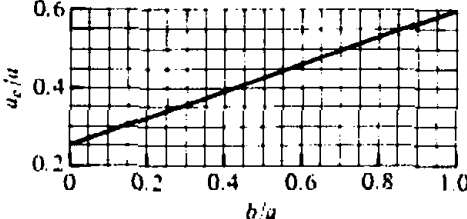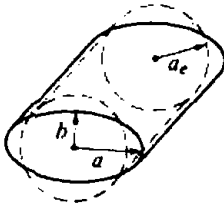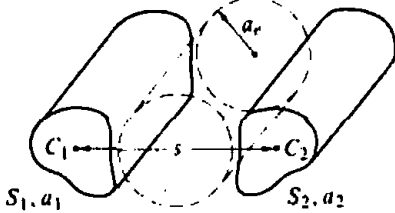
Figure 9.10 Amplitude radiation patterns of a $3\lambda/2$ dipole of various thicknesses.

input impedance, bandwidth, radiation efficiency, and effective length) coated with a layer of electrically and magnetically lossless [10] or lossy [11] medium, as shown in Figure 9.11, will be affected unless the layer is very thin compared to the radius and the wavelength. The problem was investigated analytically by the Moment Method and the effects on the radiation characteristics can be presented by defining the two parameters

$$P = \left(\frac{\dot{\epsilon}_r - 1}{\dot{\epsilon}_r}\right) \ln\left(\frac{b}{a}\right) \qquad (9\text{-}16)$$

$$Q = (\dot{\mu}_r - 1) \ln\left(\frac{b}{a}\right) \qquad (9\text{-}17)$$

Table 9.3 CONDUCTOR GEOMETRICAL SHAPES AND THEIR EQUIVALENT CIRCULAR CYLINDER RADII

Geometrical Shape	Electrical Equivalent Radius
	$a_e = 0.25a$
	$a_e \approx 0.2(a + b)$
	$a_e = 0.59a$
	$a_e = \frac{1}{2}(a + b)$
	$\ln a_e = \dfrac{1}{(S_1 + S_2)^2}$ $\times [S_1^2 \ln a_1 + S_2^2 \ln a_2 + 2S_1S_2 \ln s]$ S_1, S_2 = peripheries of conductors C_1, C_2 a_1, a_2 = equivalent radii of conductors C_1, C_2

where

$\tilde{\epsilon}_r$ = relative (to the ambient medium) complex permittivity

$\tilde{\mu}_r$ = relative (to the ambient medium) complex permeability

a = radius of the conducting wire

$b - a$ = thickness of coating

In general:

1. Increasing the real part of either P or Q
   a. increases the peak input admittance
   b. increases the electrical length (lowers the resonant frequency)
   c. narrows the bandwidth
2. Increasing the imaginary part of P or Q
   a. decreases the peak input admittance
   b. decreases the electrical length (increases the resonant frequency)
   c. increases the bandwidth
   d. accentuates the power dissipated (decreases the radiation efficiency)
   e. accentuates the traveling wave component of the current distribution

Thus the optimum bandwidth of the antenna can be achieved by choosing a lossy dielectric material with maximum imaginary parts of P and Q and minimum real parts. However, doing this decreases the radiation efficiency. In practice, a trade-off between bandwidth and efficiency is usually required. This is not a very efficient technique to broadband the antenna.
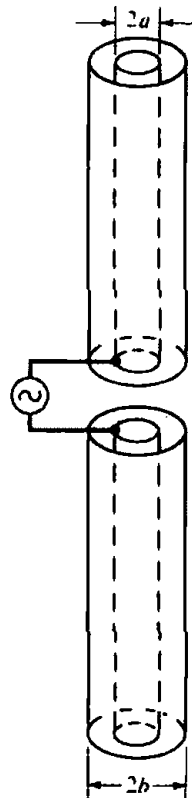

Figure 9.11 Coated linear dipole.

9.5 FOLDED DIPOLE

To achieve good directional pattern characteristics and at the same time provide good matching to practical coaxial lines with 50- or 75-ohm characteristic impedances, the length of a single wire element is usually chosen to be $\lambda/4 \leq l < \lambda$. The most widely used dipole is that whose overall length is $l \simeq \lambda/2$, and which has an input impedance of $Z_{in} \simeq 73 + j42.5$ and directivity of $D_0 \simeq 1.643$. In practice, there are other very common transmission lines whose characteristic impedance is much higher than 50 or 75 ohms. For example, a "twin lead" transmission line (usually two parallel wires separated by about $\frac{5}{16}$ in. and embedded in a low-loss plastic material used for support and spacing) is widely used for TV applications and has a characteristic impedance of about 300 ohms.

In order to provide good matching characteristics, variations of the single dipole element must be used. One simple geometry that can achieve this is a folded wire which forms a very thin ($s \ll \lambda$) rectangular loop as shown in Figure 9.12(a). This antenna, when the spacing between the two larger sides is very small (usually $s < 0.05\lambda$), is known as a folded dipole and it serves as a step-up impedance transformer (approximately by a factor of 4 when $l = \lambda/2$) of the single element impedance. Thus when $l = \lambda/2$ and the antenna is resonant, impedances on the order of about 300 ohms can be achieved, and it would be ideal for connections to "twin-lead" transmission lines.

A folded dipole operates basically as an unbalanced transmission line, and it can be analyzed by assuming that its current is decomposed into two distinct modes: a transmission line mode [Figure 9.12(b)] and an antenna mode [Figure 9.12(c)]. This type of an analytic model can be used to predict accurately the input impedance provided the longer parallel wires are close together electrically ($s \ll \lambda$).

To derive an equation for the input impedance, let us refer to the modeling of Figure 9.12. For the transmission line mode of Figure 9.12(b), the input impedance at the terminals $a - b$ or $e - f$, looking toward the shorted ends, is obtained from the impedance transfer equation

$$Z_t = Z_0 \left[\frac{Z_L + jZ_0 \tan(kl')}{Z_0 + jZ_L \tan(kl')} \right]_{\substack{l'=l/2 \\ Z_L=0}} = jZ_0 \tan\left(k\frac{l}{2}\right) \tag{9-18}$$

where Z_0 is the characteristic impedance of a two-wire transmission line

$$Z_0 = \frac{\eta}{\pi} \cosh^{-1}\left(\frac{s/2}{a}\right) = \frac{\eta}{\pi} \ln\left[\frac{s/2 + \sqrt{(s/2)^2 - a^2}}{a}\right] \tag{9-19}$$

which can be approximated for $s/2 \gg a$ by

$$Z_0 = \frac{\eta}{\pi} \ln\left[\frac{s/2 + \sqrt{(s/2)^2 - a^2}}{a}\right] = \frac{\eta}{\pi} \ln\left(\frac{s}{a}\right) = 0.733\eta \log_{10}\left(\frac{s}{a}\right) \tag{9-19a}$$

Since the voltage between the points a and b is $V/2$, and it is applied to a transmission line of length $l/2$, the transmission line current is given by

$$I_t = \frac{V/2}{Z_t} \tag{9-20}$$

For the antenna mode of Figure 9.12(c), the generator points $c - d$ and $g - h$ are each at the same potential and can be connected, without loss of generality, to form a dipole. Each leg of the dipole is formed by a pair of closely spaced wires
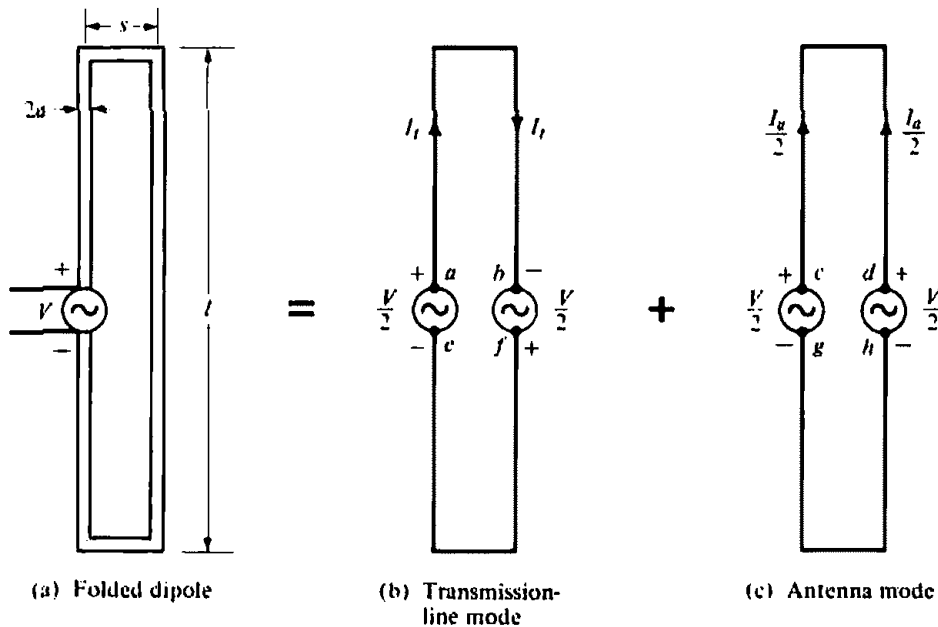
(a) Folded dipole   (b) Transmission-line mode   (c) Antenna mode

Figure 9.12 Folded dipole and its equivalent transmission line and antenna mode models. (SOURCE: G. A. Thiele, E. P. Ekelman, Jr., and L. W. Henderson, "On the Accuracy of the Transmission Line Model for Folded Dipole," *IEEE Trans. Antennas Propagat.*, Vol. AP-28, No. 5, pp. 700–703, September 1980. © (1980) IEEE)

($s \ll \lambda$) extending from the feed ($c - d$ or $g - h$) to the shorted end. Thus the current for the antenna mode is given by

$$I_a = \frac{V/2}{Z_d} \tag{9-21}$$

where Z_d is the input impedance of a linear dipole of length l and diameter d computed using (8-60a)–(8-61b). For the configuration of Figure 9.12(c), the radius that is used to compute Z_d for the dipole can be either the half-spacing between the wires ($s/2$) or an equivalent radius a_e. The equivalent radius a_e is related to the actual wire radius a by (from Table 9.3)

$$\ln(a_e) = \tfrac{1}{2}\ln(a) + \tfrac{1}{2}\ln(s) = \ln(a) + \tfrac{1}{2}\ln\!\left(\frac{s}{a}\right) = \ln\sqrt{as} \tag{9-22}$$

or

$$a_e = \sqrt{as} \tag{9-22a}$$

It should be expected that the equivalent radius yields the most accurate results.

The total current on the feed leg (left side) of the folded dipole of Figure 9.12(a) is given by

$$I_{in} = I_t + \frac{I_a}{2} = \frac{V}{2Z_t} + \frac{V}{4Z_d} = \frac{V(2Z_d + Z_t)}{4Z_t Z_d} \tag{9-23}$$

and the input impedance at the feed by

$$Z_{in} = \frac{V}{I_{in}} = \frac{2Z_t(4Z_d)}{2Z_t + 4Z_d} = \frac{4Z_t Z_d}{2Z_d + Z_t} \tag{9-24}$$
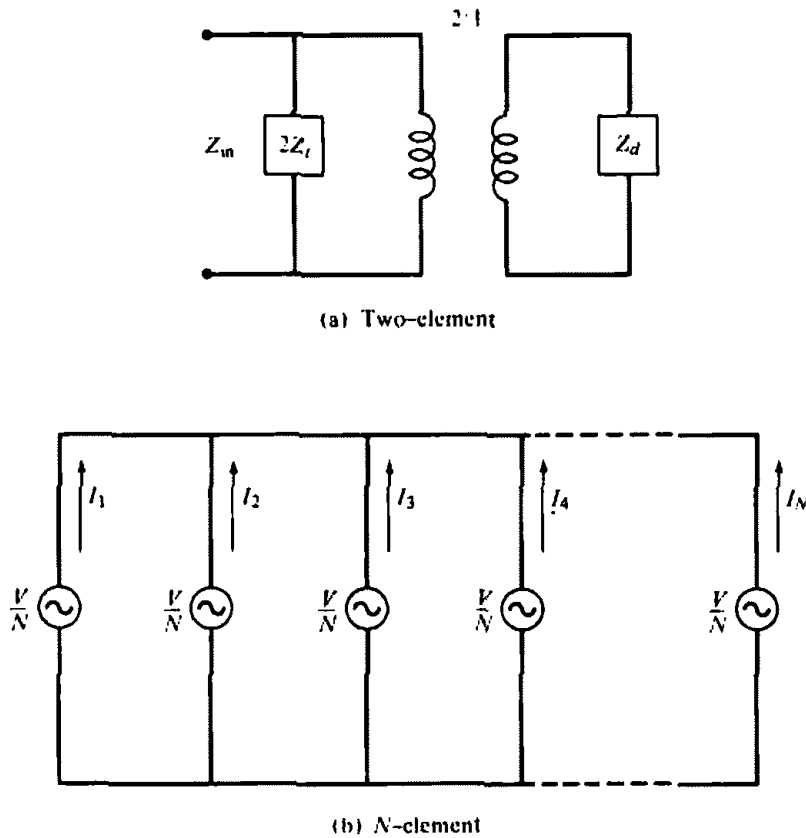
(a) Two-element

(b) N-element

Figure 9.13   Equivalent circuits for two-element and N-element (with equal radii elements) folded dipoles.

Based on (9-24), the folded dipole behaves as the equivalent of Figure 9.13(a) in which the antenna mode impedance is stepped up by a ratio of four. The transformed impedance is then placed in shunt with twice the impedance of the nonradiating (transmission line) mode to result in the input impedance.

When $l = \lambda/2$, it can be shown that (9-24) reduces to

$$\boxed{Z_{in} = 4Z_d}$$ (9-25)

or that the impedance of the folded dipole is four times greater than that of an isolated dipole of the same length as one of its sides. This is left as an exercise for the reader (Prob. 9.9).

The impedance relation of (9-25) for the $l = \lambda/2$ can also be derived by referring to Figure 9.14. Since for a folded dipole the two vertical arms are closely spaced ($s \ll \lambda$), the current distribution in each is identical as shown in Figure 9.14(a). The equivalent of the folded dipole of Figure 9.14(a) is the ordinary dipole of Figure 9.14(b). Comparing the folded dipole to the ordinary dipole, it is apparent that the currents of the two closely spaced and identical arms of the folded dipole are equal to the one current of the ordinary dipole, or

$$2I_f = I_d$$ (9-26)

where I_f is the current of the folded dipole and I_d is the current of the ordinary dipole. Also the input power of the two dipoles are identical, or

$$P_f = \frac{1}{2}I_f^2 Z_f = P_d = \frac{1}{2}I_d^2 Z_d$$ (9-27)
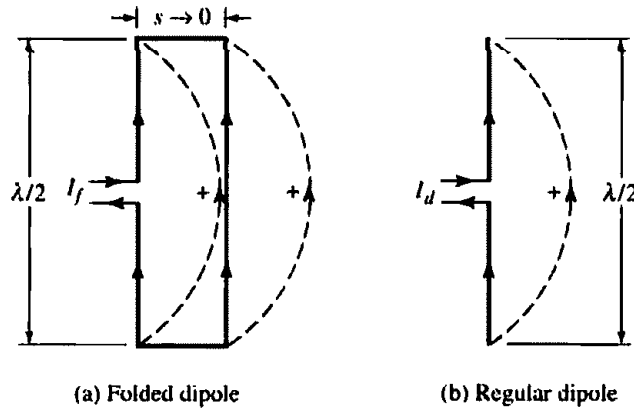
(a) Folded dipole   (b) Regular dipole

Figure 9.14 Folded dipole and equivalent regular dipole.

Substituting (9-26) into (9-27) leads to

$$Z_f = 4Z_d \tag{9-28}$$

where Z_f is the impedance of the folded dipole while Z_d is the impedance of the ordinary dipole. Equation (9-28) is identical to (9-25).

To better understand the impedance transformation of closely spaced conductors (of equal diameter) and forming a multielement folded dipole, let us refer to its equivalent circuit in Figure 9.13(b). For N elements, the equivalent voltage at the center of each conductor is V/N and the current in each is I_n, $n = 1, 2, 3, \ldots, N$. Thus the voltage across the first conductor can be represented by

$$\frac{V}{N} = \sum_{n=1}^{N} I_n Z_{1n} \tag{9-29}$$

where Z_{1n} represents the self or mutual impedance between the first and nth element. Because the elements are closely spaced

$$I_n \simeq I_1 \quad \text{and} \quad Z_{1n} \simeq Z_{11} \tag{9-30}$$

for all values of $n = 1, 2, \ldots, N$. Using (9-30), we can write (9-29) as

$$\frac{V}{N} = \sum_{n=1}^{N} I_n Z_{1n} \simeq I_1 \sum_{n=1}^{N} Z_{1n} \simeq N I_1 Z_{11} \tag{9-31}$$

or

$$\boxed{Z_{in} = \frac{V}{I_1} \simeq N^2 Z_{11} = N^2 Z_r} \tag{9-31a}$$

since the self-impedance Z_{11} of the first element is the same as its impedance Z_r in the absence of the other elements. Additional impedance step-up of a single dipole can be obtained by introducing more elements. For a three-element folded dipole with elements of identical diameters and of $l \simeq \lambda/2$, the input impedance would be about nine times greater than that of an isolated element or about 650 ohms. Greater step-up transformations can be obtained by adding more elements; in practice, they are seldom needed. Many other geometrical configurations of a folded dipole can be obtained which would contribute different values of input impedances. Small variations in impedance can be obtained by using elements of slightly different diameters and/or lengths.

To test the validity of the transmission line model for the folded dipole, a number of computations were made [12] and compared with data obtained by the Moment Method, which is considered to be more accurate. In Figures 9.15(a) and (b) the input resistance and reactance for a two-element folded dipole is plotted as a function of l/λ when the diameter of each wire is $d = 2a = 0.001\lambda$ and the spacing between the elements is $s = 0.006613\lambda$. The characteristic impedance of such a transmission line is 300 ohms. The equivalent radius was used in the calculations of Z_d. An excellent agreement is indicated between the results of the transmission line model and the Moment Method. Computations and comparisons for other spacings ($s = 0.0213\lambda$, $Z_0 = 450$ ohms and $s = 0.0742\lambda$. $Z_0 = 600$ ohms) but with elements of the same diameter ($d = 0.001\lambda$) have been made [12]. It has been shown that as the spacing between the wires increased, the results of the transmission line mode began to disagree with those of the Moment Method. For a given spacing, the accuracy for the characteristic impedance, and in turn for the input impedance, can be improved by increasing the diameter of the wires. The characteristic impedance of a transmission line, as given by (9-19) or (9-19a), depends not on the spacing but on the spacing-to-diameter (s/d) ratio, which is more accurate for smaller s/d. Computations were also made whereby the equivalent radius was not used. The comparisons of these results indicated larger disagreements, thus concluding the necessity of the equivalent radius, especially for the larger wire-to-wire spacings.

A two-element folded dipole is widely used as feed element of TV antennas such as Yagi-Uda antennas. Although the impedance of an isolated folded dipole may be around 300 ohms, its value will be somewhat different when it is used as an element in an array or with a reflector. The folded dipole has better bandwidth characteristics than a single dipole of the same size. Its geometrical arrangement tends to behave as a short parallel stub line which attempts to cancel the off resonance reactance of a single dipole. The folded dipole can be thought to have a bandwidth which is the same as that of a single dipole but with an equivalent radius ($a < a_r < s/2$).

Symmetrical and asymmetrical planar folded dipoles can also be designed and constructed using strips which can be fabricated using printed circuit technology [13]. The input impedance can be varied over a wide range of values by adjusting the width of the strips. In addition, the impedance can be adjusted to match the characteristic impedance of printed circuit transmission lines with four-to-one impedance ratios.

9.6 DISCONE AND CONICAL SKIRT MONOPOLE

There are innumerable variations to the basic geometrical configurations of cones and dipoles, some of which have already been discussed, to obtain broadband characteristics. Two other common radiators that meet this characteristic are the conical skirt monopole and the discone antenna [14] shown in Figures 9.16(a) and (b), respectively.

For each antenna, the overall pattern is essentially the same as that of a linear dipole of length $l < \lambda$ (i.e., a solid of revolution formed by the rotation of a figure-eight) whereas in the horizontal (azimuthal) plane it is nearly omnidirectional. The polarization of each is vertical. Each antenna because of its simple mechanical design, ease of installation, and attractive broadband characteristics has wide applications in the VHF (30–300 MHz) and UHF (300 MHz–3 GHz) spectrum for broadcast, television, and communication applications.

The discone antenna is formed by a disk and a cone. The disk is attached to the center conductor of the coaxial feed line, and it is perpendicular to its axis. The cone is connected at its apex to the outer shield of the coaxial line. The geometrical
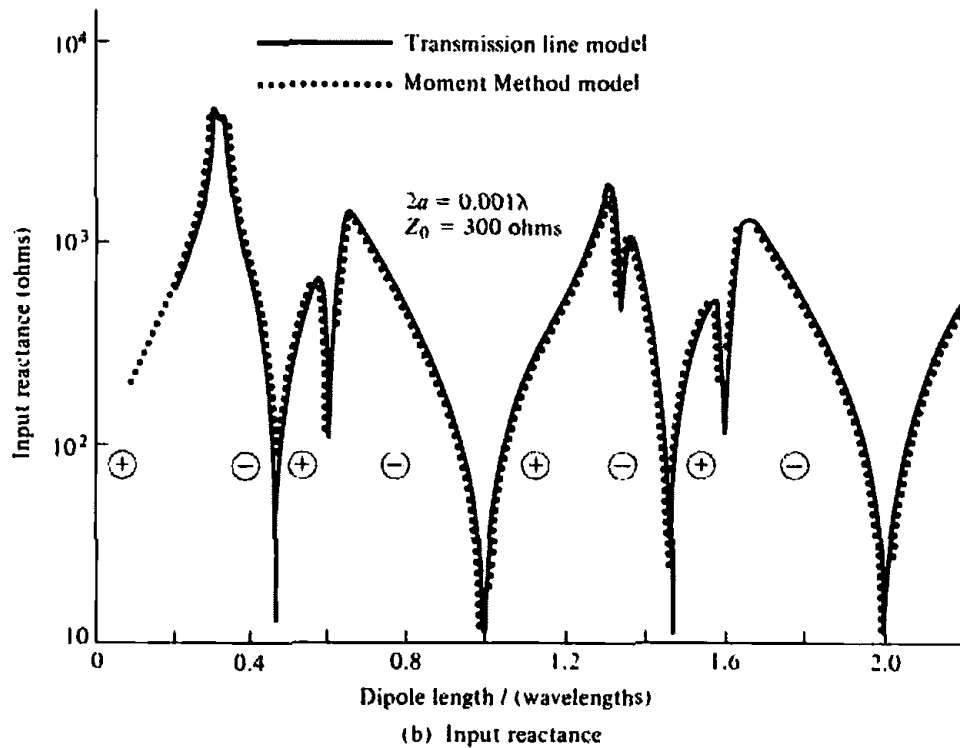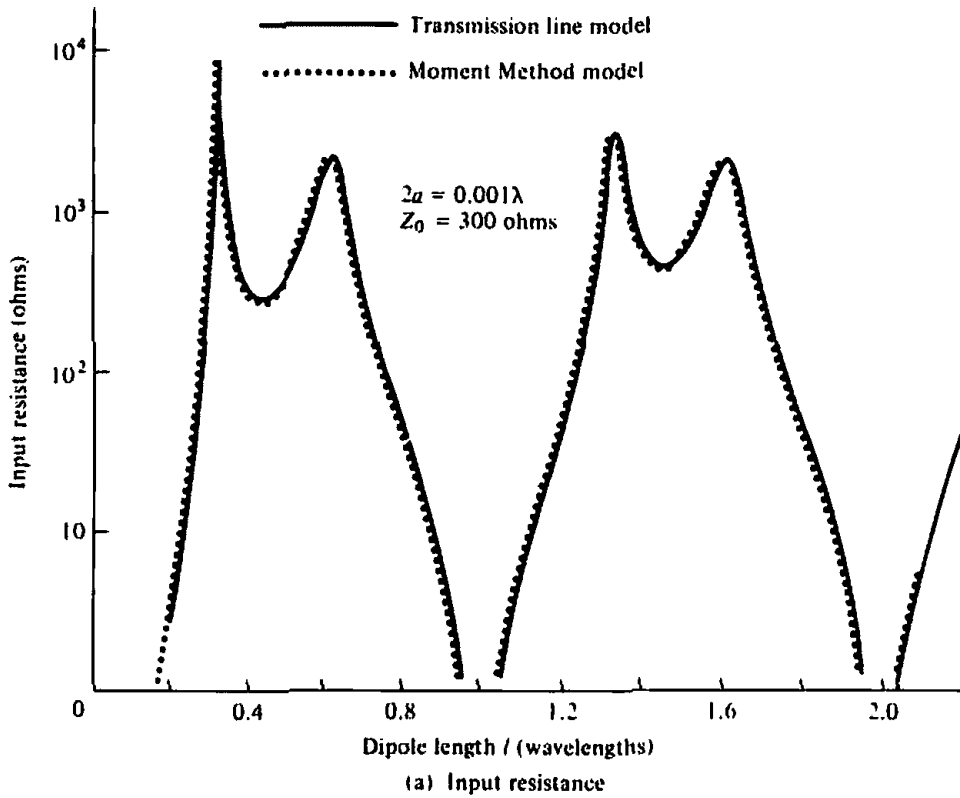
Figure 9.15   Input resistance and reactance of folded dipole. (SOURCE: G. A. Thiele, E. P. Ekelman, Jr., and L. W. Henderson. "On the Accuracy of the Transmission Line Model for Folded Dipole." *IEEE Trans. Antennas Propagat.*, Vol. AP-28, No. 5, pp. 700–703, September 1980. © (1980) IEEE)
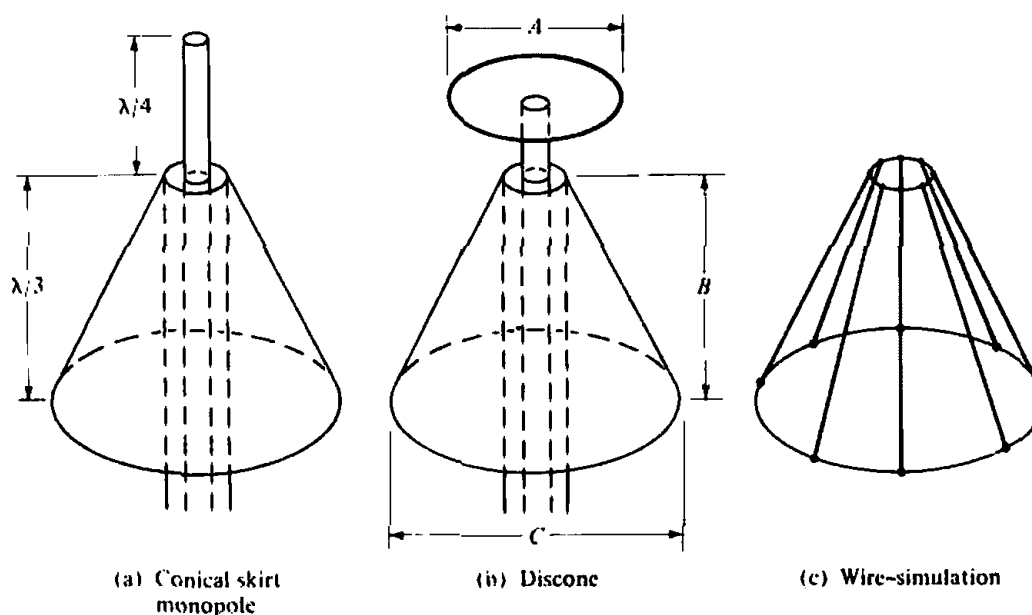
Figure 9.16 Conical skirt monopole, discone, and wire-simulated cone surface.

dimensions and the frequency of operation of two designs |14| are shown in Table 9.4.

In general, the impedance and pattern variations of a discone as a function of frequency are much less severe than those of a dipole of fixed length l. The performance of this antenna as a function of frequency is similar to a high-pass filter. Below an effective cutoff frequency it becomes inefficient, and it produces severe standing waves in the feed line. At cutoff, the slant height of the cone is approximately $\lambda/4$.

Measured elevation (vertical) plane radiation patterns from 250 to 650 MHz, at 50-MHz intervals, have been published |14| for a discone with a cutoff frequency of 200 MHz. No major changes in the "figure-eight" shape of the patterns were evident other than at the high-frequency range where the pattern began to turn downward somewhat.

The conical skirt monopole is similar to the discone except that the disk is replaced by a monopole of length usually $\lambda/4$. Its general behavior also resembles that of the discone. Another way to view the conical skirt monopole is with a $\lambda/4$ monopole mounted above a finite ground plane. The plane has been tilted downward to allow more radiation toward and below the horizontal plane.

To reduce the weight and wind resistance of the cone, its solid surface can be simulated by radial wires, as shown in Figure 9.16(c). This is a usual practice in the simulation of finite size ground planes for monopole antennas. The lengths of the wires used to simulate the ground plane are on the order of about $\lambda/4$ or greater.

9.7   SLEEVE DIPOLE

The radiation patterns of asymmetrically driven wire antennas, with overall length less than a half-wavelength ($l < \lambda/2$), will almost be independent of the point of feed along the wire. However for lengths greater than $\lambda/2$ ($l > \lambda/2$) the current variation along the wire will undergo a phase reversal while maintaining almost sinusoidal amplitude current distribution forced by the boundary conditions at its ends. It would then seem that the input impedance would largely be influenced by the feed point. Even the patterns may be influenced by the point of excitation for antennas with lengths greater than $\lambda/2$.

Table 9.4 FREQUENCY AND DIMENSIONS OF TWO
DESIGNS

Frequency (MHz)	A (cm)	B (cm)	C (cm)
90	45.72	60.96	50.80
200	22.86	31.75	35.56

The input impedance Z_{as} of an asymmetric (off-center) driven dipole is related approximately to the input impedance Z_s at its center by

$$Z_{as} \simeq \frac{Z_s}{\cos^2(k\Delta l)} \qquad (9\text{-}32)$$

where Δl represents the displacement of the feed from the center. Better accuracy can be obtained using more complicated formulas [15].

An antenna that closely resembles an asymmetric dipole and can be analyzed in a similar manner is a sleeve dipole, shown in Figure 9.17(a). This radiator is essentially the same as that of a base-driven monopole above a ground plane. The outer shield of the coaxial line. which is also connected to the ground plane, has been extended a distance l along the axis of the wire to provide mechanical strength, impedance variations, and extended broadband characteristics.

By introducing the outer sleeve, the excitation gap voltage maintained by the feeding transmission line has been moved upward from the conducting plate ($z = 0$) to $z \approx h$. The theory of images yields the equivalent symmetrical structure of Figure 9.17(b) in which two generators maintain each equal voltage at $z = \pm h$.

Because of the linearity of Maxwell's equations, the total current in the system will be equal to the sum of the currents maintained independently by each generator in each of the two asymmetric excited radiators [16] shown in Figure 9.17(c). Thus the antenna can be analyzed as the sum of two asymmetrically fed radiators, ignoring the diameter change in each as in Figure 9.17(d). Since the two structures in Figure 9.17(d) are identical at their feed, the input current is

$$I_{in} \simeq I_{as}(z = h) + I_{as}(z = -h) \qquad (9\text{-}33)$$

where

I_{in} = input current at the feed of the sleeve dipole
[Figure 9.17(a)]

$I_{as}(z = h)$ = current of asymmetric structure at $z = h$
[Figure 9.17(d)]

$I_{as}(z = -h)$ = current of asymmetric structure at $z = -h$
[Figure 9.17(d)]

and the input admittance is

$$Y_{in} = \frac{I_{as}(z = h) + I_{as}(z = -h)}{V_{in}} = \frac{I_{as}(z = h)}{V_{in}}\left[1 + \frac{I_{as}(z = -h)}{I_{as}(z = h)}\right]$$

$$= Y_{as}\left[1 + \frac{I_{as}(z = -h)}{I_{as}(z = h)}\right] \qquad (9\text{-}34)$$

where $Y_{as} = 1/Z_{as}$ as given by (9-32).

Through a number of computations [16], the frequency response of a sleeve dipole

(a) Sleeve dipole   (b) Equivalent   (c) Asymmetric   (d) Asymmetric radiators
                                        radiators equivalent   approximate equivalent
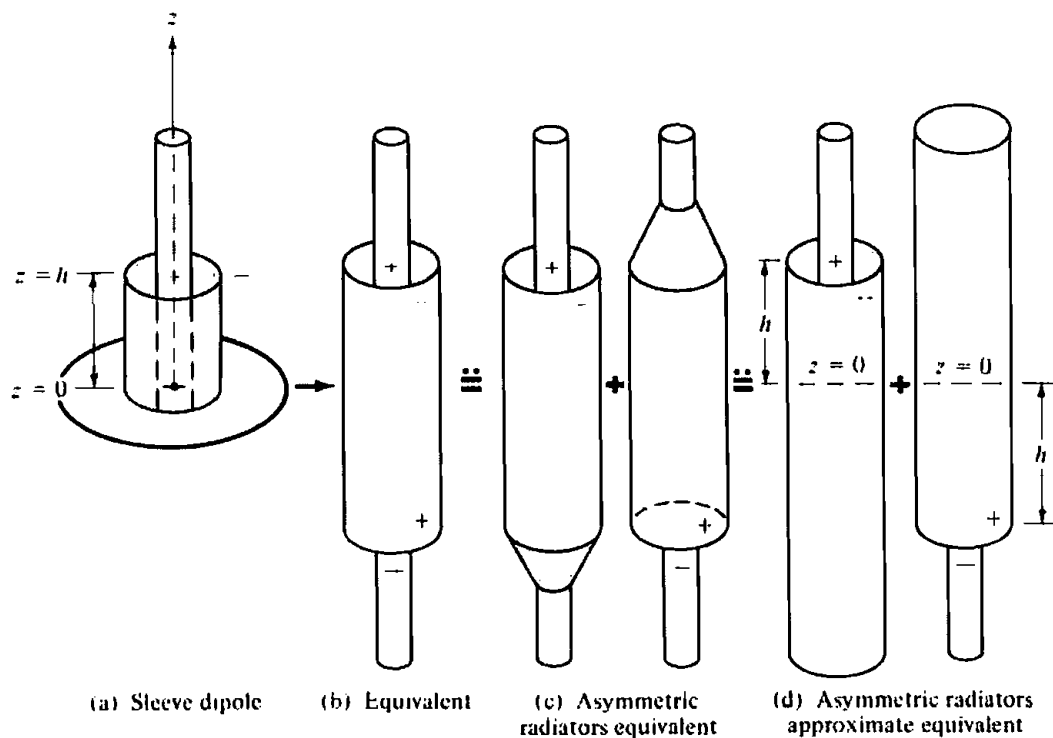
Figure 9.17   Sleeve dipole and its equivalents. (SOURCE: W. L. Weeks, *Antenna Engineering*, McGraw-Hill, New York, 1968)

has been shown to be much superior than either that of a half-wavelength or full-wavelength dipole. Also the standing wave inside the feed line can be maintained reasonably constant by the use of a properly designed reactive matching network.

9.8   MATCHING TECHNIQUES

The operation of an antenna system over a frequency range is not completely dependent upon the frequency response of the antenna element itself but rather on the frequency characteristics of the transmission line-antenna element combination. In practice, the characteristic impedance of the transmission line is usually real whereas that of the antenna element is complex. Also the variation of each as a function of frequency is not the same. Thus efficient coupling-matching networks must be designed which attempt to couple-match the characteristics of the two elements over the desired frequency range.

There are many coupling-matching networks that can be used to connect the transmission line to the antenna element and which can be designed to provide acceptable frequency characteristics. Only a limited number will be introduced here.

9.8.1   Stub-Matching

Ideal matching at a given frequency can be accomplished by placing a short- or open-circuited shunt stub a distance *s* from the transmission line-antenna element connection, as shown in Figure 9.18(a). Assuming a real characteristic impedance, the length *s* is controlled so as to make the real part of the antenna element impedance equal to the characteristic impedance. The length *l* of the shunt line is varied until the susceptance of the stub is equal in magnitude but opposite in phase to the line input susceptance at the point of the transmission line-shunt element connection. The match-

(a) Shunt matching

(b) $\lambda_0/4$ transformer

(c) N-section $\lambda_0/4$ transformer

(d) Microstrip array

(f) Microstrip (end view)

(e) Microstrip (top view)
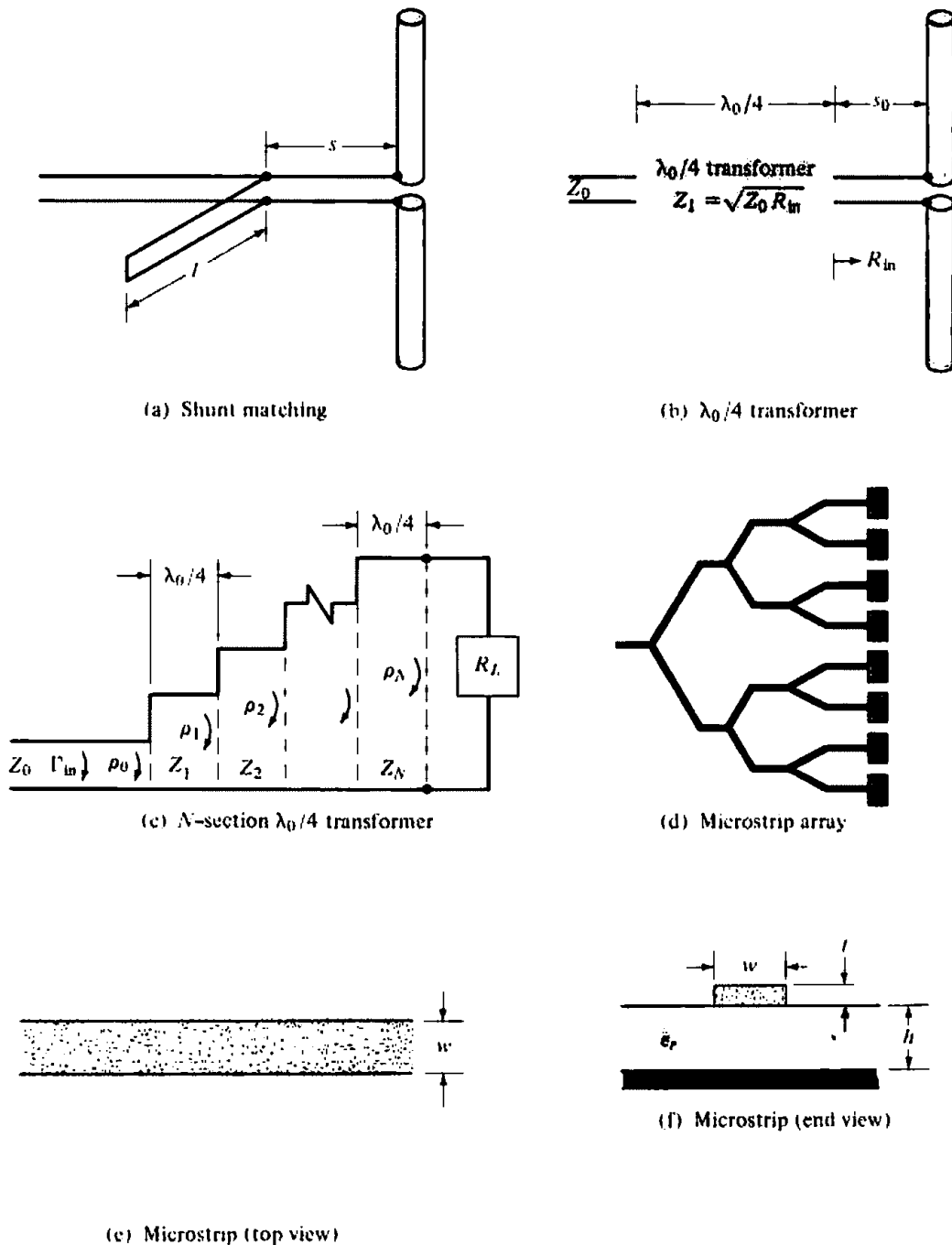
Figure 9.18 Matching and microstrip techniques.

ing procedure is illustrated best graphically with the use of a Smith chart. Analytical methods, on which the Smith chart graphical solution is based, can also be used. The short-circuited stub is more practical because an equivalent short can be created by a pin connection in a coaxial cable or a slider in a waveguide. This preserves the overall length of the stub line for matchings which may require longer length stubs.

A single stub with a variable length l cannot always match all antenna (load) impedances. A double-stub arrangement positioned a fixed distance s from the load, with the length of each stub variable and separated by a constant length d, will match a greater range of antenna impedances. However, a triple-stub configuration will always match all loads.

An excellent treatment of the analytical and graphical methods for the single-, double-, triple-stub, and other matching techniques is presented by Collin [17]. The

higher-order stub arrangements provide more broad and less sensitive matchings (to frequency variations) but are more complex to implement. Usually a compromise is chosen, such as the double-stub.

9.8.2 Quarter-Wavelength Transformer

A. Single Section

Another technique that can be used to match the antenna to the transmission line is to use a $\lambda/4$ transformer. If the impedance of the antenna is real, the transformer is attached directly to the load. However if the antenna impedance is complex, the transformer is placed a distance s_0 away from the antenna, as shown in Figure 9.18(b). The distance s_0 is chosen so that the input impedance toward the load at s_0 is real and designated as R_{in}. To provide a match, the transformer characteristic impedance Z_1 should be $Z_1 = \sqrt{R_{in}Z_0}$, where Z_0 is the characteristic impedance (real) of the input transmission line. The transformer is usually another transmission line with the desired characteristic impedance.

Because the characteristic impedances of most off-the-shelf transmission lines are limited in range and values, the quarter-wavelength transformer technique is most suitable when used with microstrip transmission lines. In microstrips, the characteristic impedance can be changed by simply varying the width of the center conductor.

B. Multiple Sections

Matchings that are less sensitive to frequency variations and that provide broader bandwidths, require multiple $\lambda/4$ sections. In fact the number and characteristic impedance of each section can be designed so that the reflection coefficient follows, within the desired frequency bandwidth, prescribed variations which are symmetrical about the center frequency. The antenna (load) impedance will again be assumed to be real; if not, the antenna element must be connected to the transformer at a point s_0 along the transmission line where the input impedance is real.

Referring to Figure 9.18(c), the total input reflection coefficient Γ_{in} for an N-section quarter-wavelength transformer with $R_L > Z_0$ can be written approximately as [17]

$$\Gamma_{in}(f) \simeq \rho_0 + \rho_1 e^{-j2\theta} + \rho_2 e^{-j4\theta} + \cdots + \rho_n e^{-j2N\theta}$$

$$= \sum_{n=0}^{N} \rho_n e^{-j2n\theta} \tag{9-35}$$

where

$$\rho_n = \frac{Z_{n+1} - Z_n}{Z_{n+1} + Z_n} \tag{9-35a}$$

$$\theta = k\Delta l = \frac{2\pi}{\lambda}\left(\frac{\lambda_0}{4}\right) = \frac{\pi}{2}\left(\frac{f}{f_0}\right) \tag{9-35b}$$

In (9-35), ρ_n represents the reflection coefficient at the junction of two infinite lines with characteristic impedances Z_n and Z_{n+1}. f_0 represents the designed center frequency, and f the operating frequency. Equation (9-35) is valid provided the ρ_n's at each junction are small ($R_L \simeq Z_0$). If $R_L < Z_0$, the ρ_n's should be replaced by $-\rho_n$'s. For a real load impedance, the ρ_n's and Z_n's will also be real.

For a symmetrical transformer ($\rho_0 = \rho_N$, $\rho_1 = \rho_{N-1}$, etc.), (9-35) reduces to

$$\Gamma_{in}(f) = 2e^{-jN\theta}[\rho_0 \cos N\theta + \rho_1 \cos(N - 2)\theta + \rho_2 \cos(N - 4)\theta + \cdots] \qquad (9\text{-}36)$$

The last term in (9-36) should be

$\rho_{[(N-1)/2]}\cos\theta$	for N = odd integer	(9-36a)
$\frac{1}{2}\rho_{(N/2)}$	for N = even integer	(9-36b)

C. Binomial Design

One technique, used to design an N-section $\lambda/4$ transformer, requires that the input reflection coefficient of (9-35) have maximally flat passband characteristics. For this method, the junction reflection coefficients (ρ_n's) are derived using the binomial expansion. Doing this, we can equate (9-35) to

$$\boxed{\begin{aligned}\Gamma_{in}(f) &= \sum_{n=0}^{N} \rho_n e^{-j2n\theta} = e^{-jN\theta} \frac{R_L - Z_0}{R_L + Z_0} \cos^N(\theta) \\ &= 2^{-N} \frac{R_L - Z_0}{R_L + Z_0} \sum_{n=0}^{N} C_n^N e^{-j2n\theta}\end{aligned}} \qquad (9\text{-}37)$$

where

$$C_n^N = \frac{N!}{(N - n)!n!}, \qquad n = 0, 1, 2, \ldots, N \qquad (9\text{-}37a)$$

From (9-35)

$$\rho_n = 2^{-N} \frac{R_L - Z_0}{R_L + Z_0} C_n^N \qquad (9\text{-}38)$$

For this type of design, the fractional bandwidth $\Delta f/f_0$ is given by

$$\frac{\Delta f}{f_0} = 2\frac{(f_0 - f_m)}{f_0} = 2\left(1 - \frac{f_m}{f_0}\right) = 2\left(1 - \frac{2}{\pi}\theta_m\right) \qquad (9\text{-}39)$$

Since

$$\theta_m = \frac{2\pi}{\lambda_m}\left(\frac{\lambda_0}{4}\right) = \frac{\pi}{2}\left(\frac{f_m}{f_0}\right) \qquad (9\text{-}40)$$

(9-39) reduces using (9-37) to

$$\frac{\Delta f}{f_0} = 2 - \frac{4}{\pi}\cos^{-1}\left[\frac{\rho_m}{(R_L - Z_0)/(R_L + Z_0)}\right]^{1/N} \qquad (9\text{-}41)$$

where ρ_m is the maximum value of reflection coefficient which can be tolerated within the bandwidth.

The usual design procedure is to specify the

1. load impedance (R_L)
2. input characteristic impedance (Z_0)
3. number of sections (N)
4. maximum tolerable reflection coefficient (ρ_m) [or fractional bandwidth ($\Delta f/f_0$)]

and to find the

1. characteristic impedance of each section
2. fractional bandwidth [or maximum tolerable reflection coefficient (ρ_m)]

To illustrate the principle, let us consider an example.

Example 9.1

A linear dipole with an input impedance of $70 + j37$ is connected to a 50-ohm line. Design a two-section $\lambda/4$ binomial transformer by specifying the characteristic impedance of each section to match the antenna to the line at $f = f_0$. If the input impedance (at the point the transformer is connected) is assumed to remain constant as a function of frequency, determine the maximum reflection coefficient and VSWR within a fractional bandwidth of 0.375.

SOLUTION

Since the antenna impedance is not real, the antenna must be connected to the transformer through a transmission line of length s_0. Assuming a 50-ohm characteristic impedance for that section of the transmission line, the input impedance at $s_0 = 0.062\lambda$ is real and equal to 100 ohms. Using (9-37a) and (9-38)

$$\rho_n = 2^{-N}\frac{R_L - Z_0}{R_L + Z_0}C_n^N \approx 2^{-N}\frac{R_L - Z_0}{R_L + Z_0}\frac{N!}{(N-n)!n!}$$

which for $N = 2$, $R_L = 100$, $Z_0 = 50$

$$n = 0: \quad \rho_0 = \frac{Z_1 - Z_0}{Z_1 + Z_0} = \frac{1}{12} \Rightarrow Z_1 = 1.182Z_0 = 59.09$$

$$n = 1: \quad \rho_1 = \frac{Z_2 - Z_1}{Z_2 + Z_1} = \frac{1}{6} \Rightarrow Z_2 = 1.399Z_1 = 82.73$$

For a fractional bandwidth of 0.375 ($\theta_m = 1.276$ rad $= 73.12°$) we can write, using (9-41)

$$\frac{\Delta f}{f_0} = 0.375 = 2 - \frac{4}{\pi}\cos^{-1}\left[\frac{\rho_m}{(R_L - Z_0)/(R_L + Z_0)}\right]^{1/2}$$

which for $R_L = 100$ and $Z_0 = 50$ gives

$$\rho_m = 0.028$$

The maximum voltage standing wave ratio is

$$VSWR_m = \frac{1 + \rho_m}{1 - \rho_m} = 1.058$$

The magnitude of the reflection coefficient is given by (9-37) as

$$\Gamma_{in} = \rho_{in} = \left|\frac{R_L - Z_0}{R_L + Z_0}\right|\cos^2\theta = \frac{1}{3}\cos^2\left[\frac{2\pi}{\lambda}\left(\frac{\lambda_0}{4}\right)\right] = \frac{1}{3}\cos^2\left[\frac{\pi}{2}\left(\frac{f}{f_0}\right)\right]$$

which is shown plotted in Figure 9.19, and it is compared with the response of a single section $\lambda/4$ transformer.
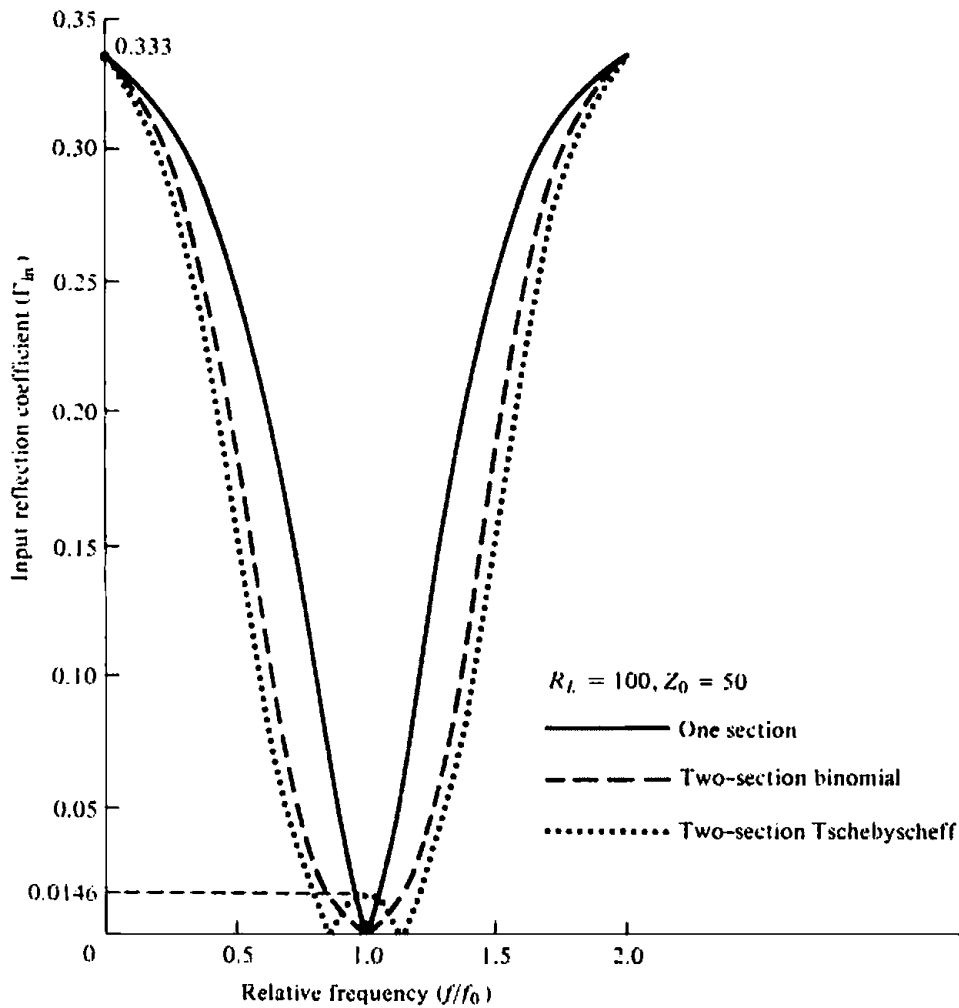
Figure 9.19 Responses of single-section, and two-section binomial and Tschebyscheff quarter-wavelength transformers.

Microstrip designs are ideally suited for antenna arrays, as shown in Figure 9.18(d). In general the characteristic impedance of a microstrip line, whose top and end views are shown in Figures 9.18(e) and (f), respectively, is given by [18].

$$Z_c = \frac{87}{\sqrt{\epsilon_r + 1.41}} \ln\left(\frac{5.98h}{0.8w + t}\right) \qquad \text{for } h < 0.8w \qquad (9\text{-}42)$$

where

ϵ_r = dielectric constant of dielectric substrate (board material)

h = height of substrate

w = width of microstrip center conductor

t = thickness of microstrip center conductor

Thus for constant values of ϵ_r, h, and t, the characteristic impedance can be changed by simply varying the width (w) of the center conductor.

D. Tschebyscheff Design

The reflection coefficient can be made to vary within the bandwidth in an oscillatory manner and have equal-ripple characteristics. This can be accomplished by making

Γ_{in} behave according to a Tschebyscheff polynomial. For the Tschebyscheff design, the equation that corresponds to (9-37) is

$$\Gamma_{in}(f) = e^{-jN\theta} \frac{Z_L - Z_0}{Z_L + Z_0} \frac{T_N(\sec\theta_m \cos\theta)}{T_N(\sec\theta_m)}$$ (9-43)

where $T_N(x)$ is the Tschebyscheff polynomial of order N.

The maximum allowable reflection coefficient occurs at the edges of the passband where $\theta = \theta_m$ and $T_N(\sec\theta_m \cos\theta)|_{\theta=\theta_m} = 1$. Thus

$$\rho_m = \left| \frac{Z_L - Z_0}{Z_L + Z_0} \frac{1}{T_N(\sec\theta_m)} \right|$$ (9-44)

The first few Tschebyscheff polynomials are given by (6-69). For $z = \sec\theta_m \cos\theta$, the first three polynomials reduce to

$$T_1(\sec\theta_m \cos\theta) = \sec\theta_m \cos\theta$$

$$T_2(\sec\theta_m \cos\theta) = 2(\sec\theta_m \cos\theta)^2 - 1 = \sec^2\theta_m \cos 2\theta + (\sec^2\theta_m - 1)$$

$$T_3(\sec\theta_m \cos\theta) = 4(\sec\theta_m \cos\theta)^3 - 3(\sec\theta_m \cos\theta)$$ (9-45)

$$= \sec^3\theta_m \cos 3\theta + 3(\sec^3\theta_m - \sec\theta_m)\cos\theta$$

The remaining details of the analysis are found in [17].

The design of Example 9.1 using a Tschebyscheff transformer is assigned as an exercise to the reader (Prob. 9.17). However its response is shown plotted in Figure 9.19 for comparison.

In general, the multiple sections (either binomial or Tschebyscheff) provide greater bandwidths than a single section. As the number of sections increases, the bandwidth also increases. The advantage of the binomial design is that the reflection coefficient values within the bandwidth monotonically decrease from both ends toward the center. Thus the values are always smaller than an acceptable and designed value that occurs at the "skirts" of the bandwidth. For the Tschebyscheff design, the reflection coefficient values within the designed bandwidth are equal or smaller than an acceptable and designed value. The number of times the reflection coefficient reaches the maximum ripple value within the bandwidth is determined by the number of sections. In fact, for an even number of sections the reflection coefficient at the designed center frequency is equal to the maximum allowable value, while for an odd number of sections it is zero. For a maximum tolerable reflection coefficient, the N-section Tschebyscheff transformer provides a larger bandwidth than a corresponding N-section binomial design, or for a given bandwidth the maximum tolerable reflection coefficient is smaller for a Tschebyscheff design.

9.8.3 T-Match

Another effective shunt-matching technique is the T-match connection shown in Figure 9.20(a). With this method the dipole of length l and radius a is connected to the transmission line by another dipole of length l' ($l' < l$) and radius a'. The smaller dipole is "tapped" to the larger one at distances $l'/2$ from the center and the two are separated by a small distance s. The transmission line is connected to the smaller dipole at its center. The T-match connection is a general form of a folded dipole since the two legs are usually not of the same length or diameter. Since the T-match is a

(a) T-match

(b) Shorted transmission line equivalent

(c) Two-wire transmission line

(d) Equivalent circuit for T-match

(e) T-match resonant connection

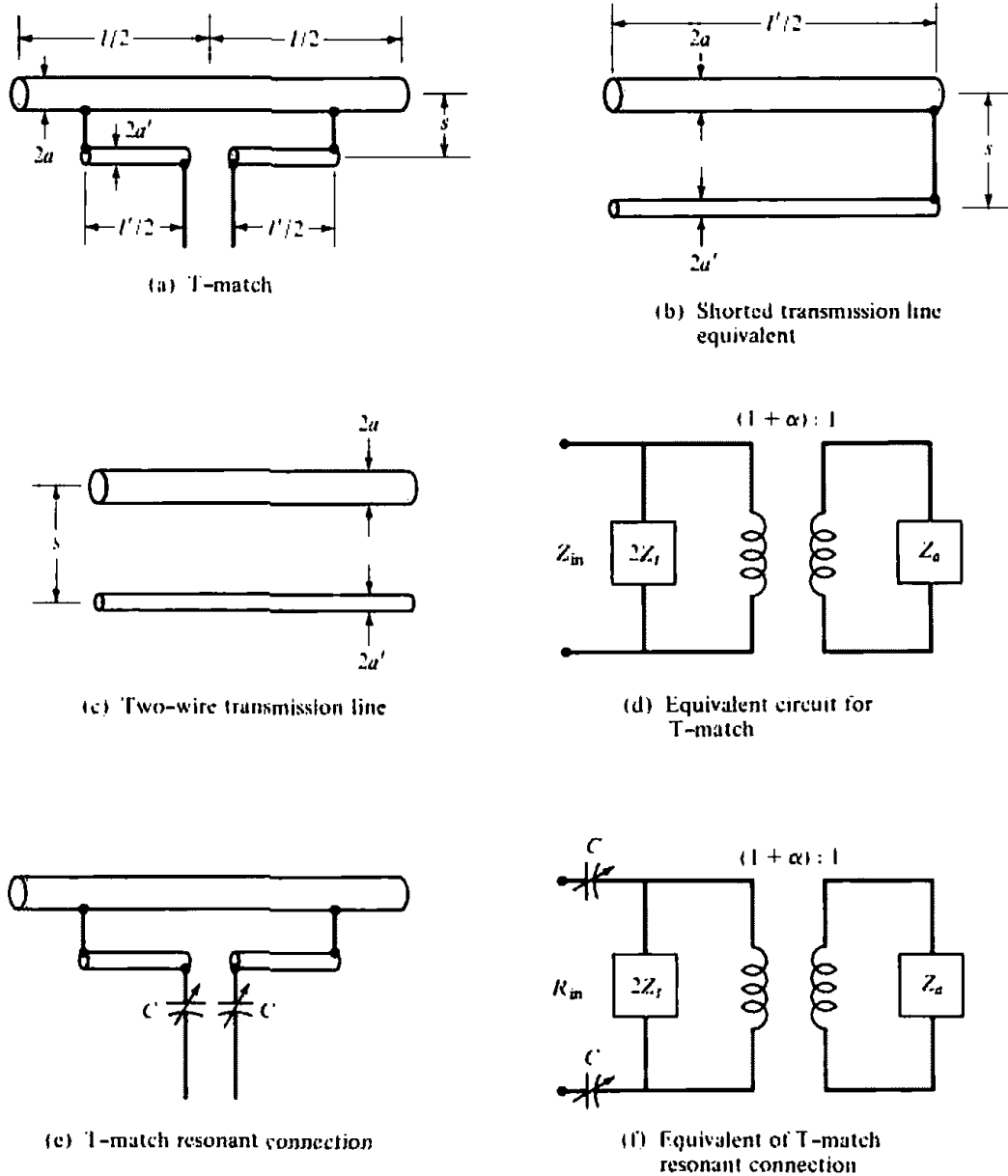(f) Equivalent of T-match resonant connection

Figure 9.20 T-match and its associated equivalents.

symmetrical and balanced system, it is well suited for use with parallel-conductor transmission lines such as the "twin lead." Coaxial lines, which are unsymmetrical and unbalanced lines, should be connected to dipoles using the gamma match.

The design procedure for the T-match is developed similarly to that of the folded dipole. The T-match is also modeled by transmission line and antenna modes, as shown in Figure 9.12 for the folded dipole. The total current at the input terminals is divided between the two conductors in a way that depends on the relative radii of the two conductors and the spacing between them. Since the two conductors are not in general of the same radius, the antenna mode current division is not unity. Instead, a current division factor is assigned which also applies to the voltage division of the transmission line mode.

Instead of including all the details of the analysis, only the steps that are applicable to a T-match design will be included.

A. Design Procedure

1. Calculate the current division factor α by

$$\alpha = \frac{\cosh^{-1}\left(\dfrac{v^2 - u^2 + 1}{2v}\right)}{\cosh^{-1}\left(\dfrac{v^2 + u^2 - 1}{2vu}\right)} \simeq \frac{\ln(v)}{\ln(v) - \ln(u)} \tag{9-46}$$

$$u = \frac{a}{a'} \tag{9-46a}$$

$$v = \frac{s}{a'} \tag{9-46b}$$

2. From Table 9.3, the "equivalent" radius of the two-wire arrangement can be written as

$$\ln(a_e) \simeq \frac{1}{(a' + a)^2}[a'^2 \ln a' + a^2 \ln a + 2a'a \ln s] \tag{9-47}$$

since $S_1 = 2\pi a'$, $S_2 = 2\pi a$. It can be shown that (9-47) reduces to

$$\ln(a_e) \simeq \ln a' + \frac{1}{(1 + u)^2}(u^2 \ln u + 2u \ln v) \tag{9-47a}$$

3. Calculate the impedance at the input terminals for the transmission line mode [i.e., two-wire shorted transmission line of length $l'/2$ with radii a, a' and separation s shown in Figure 9.20(b)]

$$Z_t = jZ_0 \tan\left(k\frac{l'}{2}\right) \tag{9-48}$$

where

$$Z_0 = 60 \cosh^{-1}\left(\frac{s^2 - a^2 - a'^2}{2aa'}\right) \simeq 276 \log_{10}\left(\frac{s}{\sqrt{aa'}}\right) \tag{9-48a}$$

Z_0 is the characteristic impedance of the two-wire transmission line with radii a, a' and separation s, as shown in Figure 9.20(c).

4. The total input impedance, which is a combination of the antenna (radiating) and the transmission (nonradiating) modes, can be written as

$$Z_{in} = R_{in} + jX_{in} = \frac{2Z_t[(1 + \alpha)^2 Z_a]}{2Z_t + (1 + \alpha)^2 Z_a} \tag{9-49}$$

and the input admittance as

$$Y_{in} = \frac{1}{Z_{in}} = \frac{Y_a}{(1 + \alpha)^2} + \frac{1}{2Z_t} \tag{9-50}$$

$Z_a = 1/Y_a$ is the center point free-space input impedance of the antenna in the absence of the T-match connection.

B. Equivalent Circuit

Based upon (9-49) or (9-50), the T-match behaves as the equivalent circuit of Figure 9.20(d) in which the antenna impedance is stepped up by a ratio of $1 + \alpha$,

and it is placed in shunt with twice the impedance of the nonradiating mode (transmission line) to result in the input impedance. When the current division factor is unity $(\alpha = 1)$, the T-match equivalent of Figure 9.20(d) reduces to that of Figure 9.14(a) for the folded dipole.

For $l' = \lambda/2$, the transmission line impedance Z_t is much greater than $(1 + \alpha)^2 Z_a$ and the input impedance of (9-49) reduces to

$$Z_{in} \simeq (1 + \alpha)^2 Z_a \qquad (9\text{-}51)$$

For two equal radii conductors, the current division factor is unity and (9-51) becomes

$$Z_{in} \simeq 4Z_a \qquad (9\text{-}52)$$

a relation obtained previously.

The impedance of (9-49) is generally complex. Because each of the lengths $(l'/2)$ of the T-match rods are usually selected to be very small $(0.03$ to $0.06\lambda)$, Z_{in} is inductive. To eliminate the reactance (resonate the antenna) at a given center frequency and keep a balanced system, two variable series capacitors are usually used, as shown in Figure 9.20(e). The value of each capacitor is selected so that Z_{in} of (9-49) is equal to $R_{in}(Z_{in} = R_{in})$. To accomplish this

$$C = 2C_{in} = \frac{1}{\pi f X_{in}} \qquad (9\text{-}53)$$

where f is the center frequency, and C_{in} is the series combination of the two C capacitors. The resonant circuit equivalent is shown in Figure 9.20(f).

The T-match connection of Figure 9.20(e) is used not only to resonate the circuit, but also to make the total input impedance equal to the characteristic impedance of the feed transmission line. This is accomplished by properly selecting the values of $l'/2$ and C (s is not usually varied because the impedance is not very sensitive to it). In most cases, a trial and error procedure is followed. An orderly graphical method using the Smith chart is usually more convenient, and it is demonstrated in the following section for the gamma match.

9.8.4 Gamma Match

Frequently dipole antennas are fed by coaxial cables which are unbalanced transmission lines. A convenient method to connect the dipole or other antennas (Yagi-Uda, log-periodic, etc.) to 50- or 75-ohm "coaxs" and to obtain a match is to use the gamma match arrangement shown in Figure 9.21.

A. Equivalent Circuit

The gamma match is equivalent to half of the T-match, and it also requires a capacitor in series with the gamma rod. The equivalent is shown in Figure 9.21(b). and its input impedance is equal to

$$Z_{in} = -jX_c + \frac{Z_g[(1 + \alpha)^2 Z_a]}{2Z_g + (1 + \alpha)^2 Z_a} \qquad (9\text{-}54)$$

where Z_a is the center point free-space impedance of the antenna in the absence of the gamma match connection. The second term of (9-54) is similar in form to that of (9-49).

The usual problem encountered is that the length of the wire antenna (l) and the
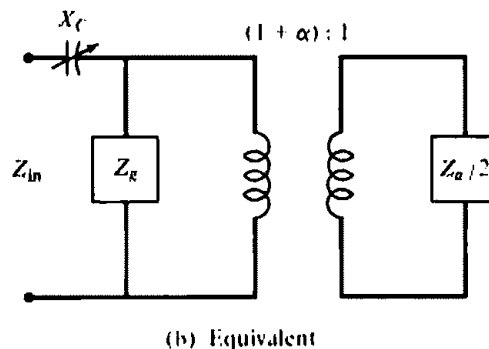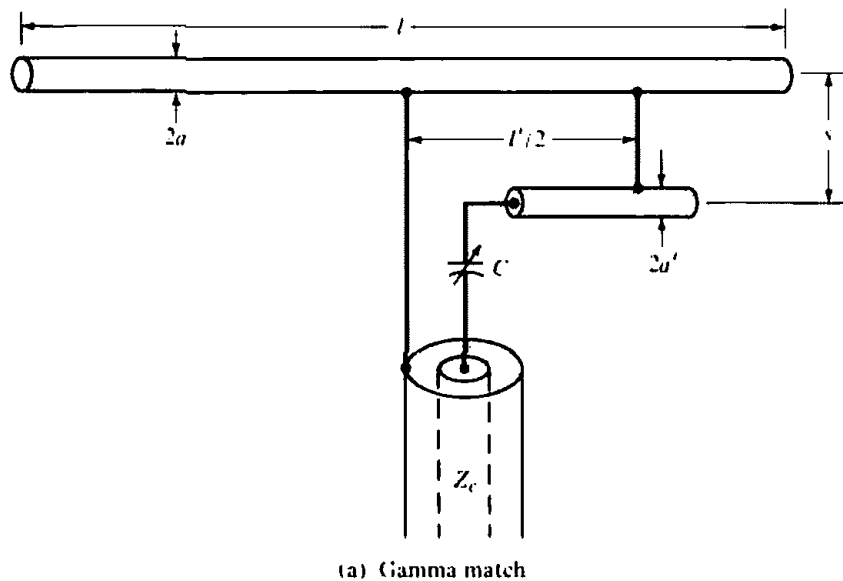
Figure 9.21   Gamma match and its equivalent.

characteristic impedance of the feed coax (Z_c) are known. What is required are the values of the radii a and a', the length $l'/2$, and the capacitance C which will achieve a match. Since the arrangement is similar to the T-match or folded dipole, its analysis is based on the same theory.

To accomplish the match, a graphical design technique, which is different from that reported in [19] and [20], will be demonstrated. This procedure utilizes the Smith chart, and it is based on the equivalent of Figure 9.21(b). A purely mathematical procedure is also available [21], but it will not be included here.

Because the input impedance is not very sensitive to a, a', and s, the usual procedure is to select their values and keep them fixed. The parameters that are usually varied are then $l'/2$ and C. In practice, $l'/2$ is varied by simply using a sliding clamp to perform the shorted connection at the end of the gamma rod.

The graphical design method assumes that $l'/2$ is given, and C that resonates the circuit is found. If the input resistance is not equal to the characteristic impedance Z_c of the feed line, another value of $l'/2$ is selected, and the procedure is repeated until $R_{in} = Z_c$. The graphical method is suggestive as to how the length $l'/2$ should be changed (smaller or larger) to accomplish the match.

B. Design Procedure

1. Determine the current division factor α by using (9-46)–(9-46b).
2. Find the free-space impedance (in the absence of the gamma match) of the driven element at the center point. Designate it as Z_a.

3. Divide Z_a by 2 and multiply it by the step-up ratio $(1 + \alpha)^2$. Designate the result as Z_2.

$$Z_2 = R_2 + jX_2 = (1 + \alpha)^2 \frac{Z_a}{2}$$ (9-55)

4. Determine the characteristic impedance Z_0 of the transmission line formed by the driven element and the gamma rod using (9-48a).

5. Normalize Z_2 of (9-55) by Z_0 and designate it as z_2.

$$z_2 = \frac{Z_2}{Z_0} = \frac{R_2 + jX_2}{Z_0} = r_2 + jx_2$$ (9-56)

and enter on the Smith chart.

6. Invert z_2 of (9-56) and obtain its equivalent admittance $y_2 = g_2 + jb_2$. On the Smith chart this is accomplished by moving z_2 diagonally across from its position.

7. In shunt with the admittance y_2 from step 6 is an inductive reactance due to the short-circuited transmission line formed by the antenna element and the gamma rod. This is an inductive reactance because the length of the gamma rod is very small (usually 0.03 to 0.06λ), but always much smaller than $\lambda/2$. Obtain its normalized value using

$$z_g = j \tan\left(k \frac{l'}{2}\right)$$ (9-57)

and place on Smith chart. The impedance z_g of (9-57) can also be obtained by using exclusively the Smith chart. You begin by locating the short-circuited load at $Z_s = 0 + j0$. Then you move this point a distance $l'/2$ toward the generator, along the outside perimeter of the Smith chart. The new point represents the normalized impedance z_g of (9-57).

8. Invert the impedance from step 7 (z_g) to obtain its equivalent admittance $y_g = g_g + jb_g$. On the Smith chart this is accomplished by moving z_g diagonally across from its position.

9. Add the two parallel admittances (from steps 6 and 8) to obtain the total input admittance at the gamma feed. That is,

$$y_{in} = y_2 + y_g = (g_2 + g_g) + j(b_2 + b_g)$$ (9-58)

and locate it on the Smith chart.

10. Invert the normalized input admittance y_{in} of (9-58) to obtain the equivalent normalized input impedance

$$z_{in} = r_{in} + jx_{in}$$ (9-59)

11. Obtain the unnormalized input impedance by multiplying z_{in} by Z_0.

$$Z_{in} = R_{in} + jX_{in} = Z_0 z_{in}$$ (9-60)

12. Select the capacitor C so that its reactance is equal in magnitude to X_{in}.

$$\frac{1}{\omega C} = \frac{1}{2\pi f_0 C} = X_{in}$$ (9-61)

If all the dimensions were chosen properly for a perfect match, the real part R_{in} of (9-60) should be equal to Z_c. If not, change one or more of the dimensions

(usually the length of the rod) and repeat the procedure until $R_{in} = Z_c$. Practically the capacitor C is chosen to be variable so adjustments can be made with ease to obtain the best possible match.

Example 9.2

The driven element impedance of a 20-m ($f = 15$ MHz; see Appendix VIII) Yagi-Uda antenna has a free-space impedance at its center point of $30.44(1 - j)$ ohms [20]. It is desired to connect it to a 50-ohm coaxial line using a gamma match. The driven element and the gamma rod are made of tubing with diameters of $0.95 \times 10^{-3}\lambda$ (0.75 in. $= 1.905$ cm) and $3.175 \times 10^{-4}\lambda$ (0.25 in. $= 0.635$ cm), respectively. The center-to-center separation between the driven element and the rod is $3.81 \times 10^{-3}\lambda$ (3 in. $= 7.62$ cm). Determine the required capacitance to achieve a match. Begin with a gamma rod length of 0.036λ (28.35 in. $= 72.01$ cm).

SOLUTION

1. Using (9-46)–(9-46b)

$$u = \frac{a}{a'} = 3 \qquad v = \frac{s}{a'} = \frac{3.81}{0.15875} = 24$$

$$\alpha \simeq \frac{\ln(24)}{\ln(24) - \ln(3)} = 1.528$$

and the step-up ratio

$$(1 + \alpha)^2 = (1 + 1.528)^2 = 6.39$$

2. $Z_a = 30.44(1 - j)$, as given.
3. Using (9-55)

$$Z_2 = (1 + 1.528)^2 \frac{30.44(1 - j)}{2} = 97.25(1 - j)$$

4. $Z_0 = 276 \log_{10}\left[\frac{2(3.81)}{\sqrt{0.95(0.3175)}}\right] = 315.25 \simeq 315$

5. $z_2 = \frac{97.25}{315}(1 - j) = 0.31(1 - j)$

6. On the Smith chart in Figure 9.22 locate z_2 and invert it to y_2. It leads to

$$y_2 = \frac{1}{z_2} = 1.6(1 + j)$$

7. On the Smith chart locate $z_s = 0 + j0$ and advance it toward the generator a distance 0.036λ to obtain

$$z_g = 0 + j0.23$$

8. From the Smith chart
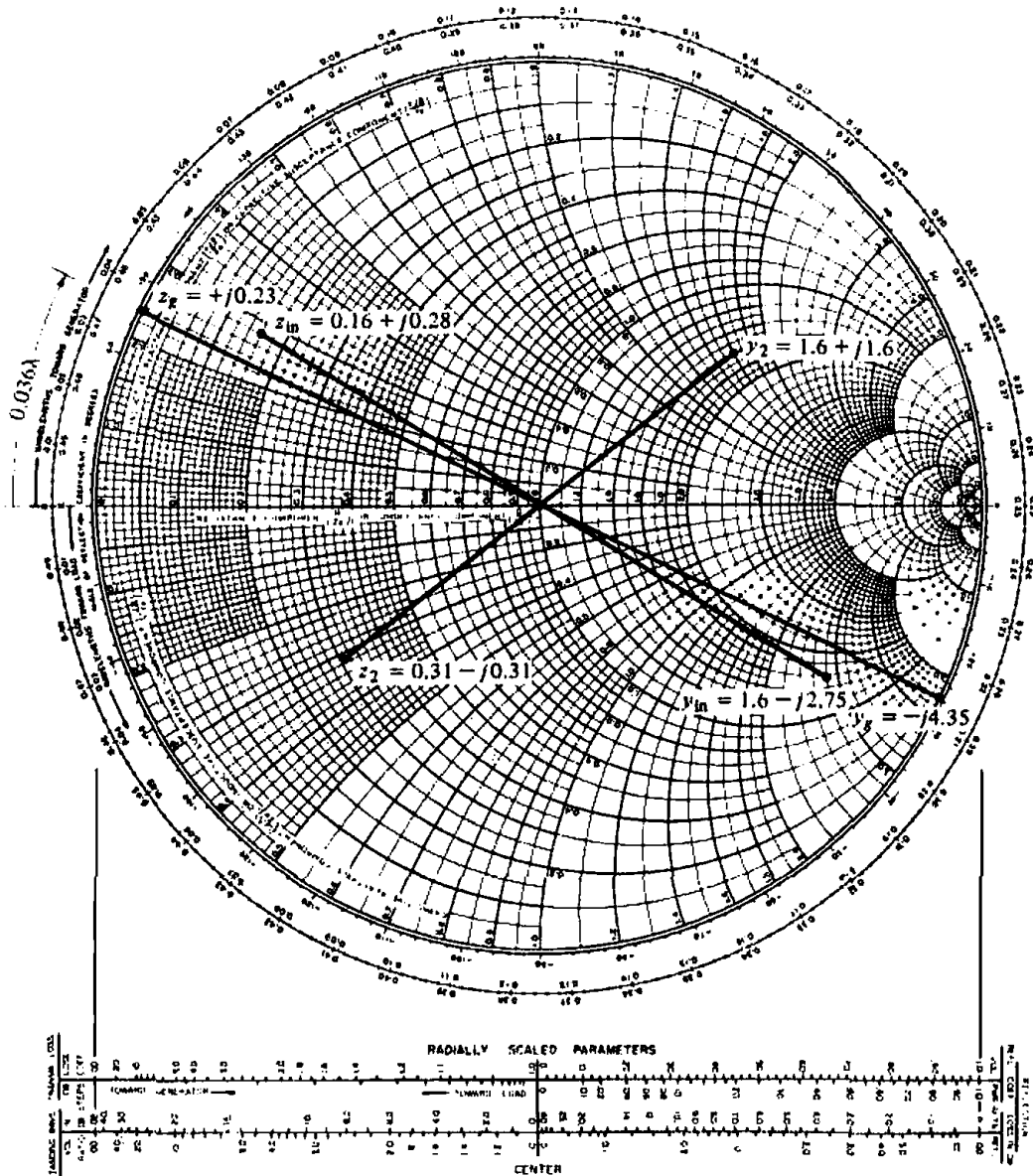
$$y_g = \frac{1}{z_g} = -j4.35$$

Figure 9.22 Smith chart for Example 9.2. Copyright renewal 1976 by P. H. Smith, Murray Hill, N.J.

9. Add y_2 and y_g

$$y_{in} = y_2 + y_g = 1.6 - j2.75$$

which is located on the Smith chart.

10. Inverting y_{in} on the Smith chart to z_{in} gives

$$z_{in} = 0.16 + j0.28$$

11. Unnormalizing z_{in} by $Z_0 = 315$. reduces it to

$$Z_{in} = 50.4 + j88.2$$

12. The capacitance should be

$$C = \frac{1}{2\pi f_0(88.2)} = \frac{1}{2\pi(15 \times 10^6)(88.2)}$$

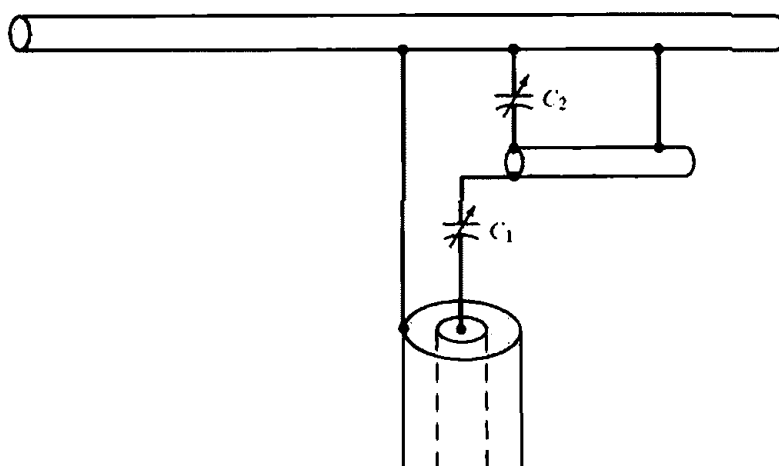$$= 120.3 \times 10^{-12} = 120 \text{ pF}$$

Figure 9.23   Omega match arrangement.

Since R_{in} = 50.4 ohms is not exactly equal to Z_0 = 50 ohms, one of the physical dimensions (usually the length of the rod) can be changed slightly and then the process can be repeated. However in this case they are so close that for practical purposes this is not required.

9.8.5 Omega Match

A slightly modified version of the gamma match is the omega match shown in Figure 9.23. The only difference between the two is that in addition to the series capacitor C_1 there is one in shunt C_2 which can aid in achieving the match. Usually the presence of C_2 makes it possible to use a shorter rod or makes it easier to match a resonant driven element. The primary function of C_2 is to change y_{in} in step 9 of the design procedure so that when it is inverted its unnormalized real part is equal to the characteristic impedance of the input transmission line. This will possibly eliminate the need of changing the dimensions of the matching elements. if a match is not achieved.

9.8.6 Baluns and Transformers

A twin-lead transmission line (two parallel-conductor line) is a symmetrical line whereas a coaxial cable is inherently unbalanced. Because the inner and outer (inside and outside parts of it) conductors of the coax are not coupled to the antenna in the same way, they provide the unbalance. The result is a net current flow to ground on the outside part of the outer conductor. This is shown in Figure 9.24(a) where an electrical equivalent is also indicated. The amount of current flow I_3 on the outside surface of the outer conductor is determined by the impedance Z_g from the outer shield to ground. If Z_g can be made very large, I_3 can be reduced significantly. Devices that can be used to balance inherently unbalanced systems. by canceling or choking the outside current. are known as *baluns* (*bal*ance to *un*balance).

One type of a balun is that shown in Figure 9.24(b), referred to usually as a *bazooka* balun. Mechanically it requires that a $\lambda/4$ in length metal sleeve, and shorted at its one end, encapsulates the coaxial line. Electrically the input impedance at the open end of this $\lambda/4$ shorted transmission line, which is equivalent to Z_g, will be very large (ideally infinity). Thus the current I_3 will be choked, if not completely eliminated, and the system will be nearly balanced.

(a) Unbalanced coaxial line
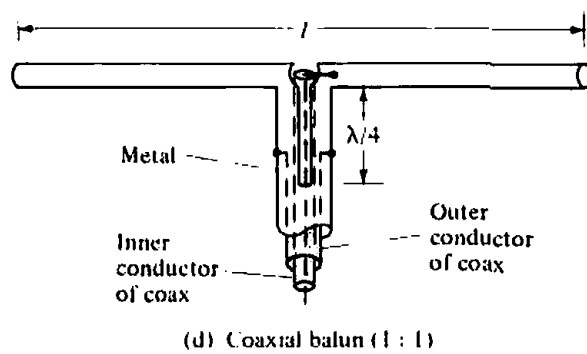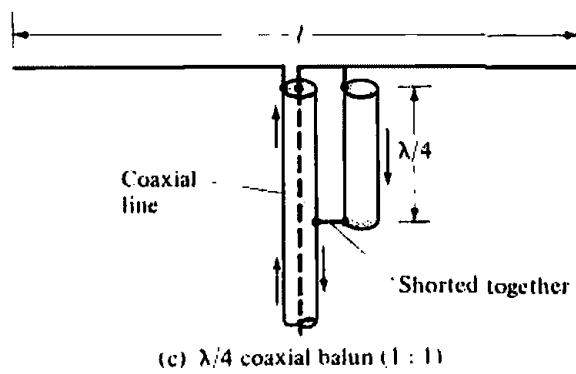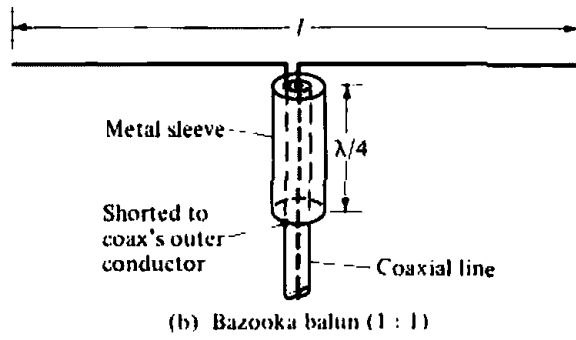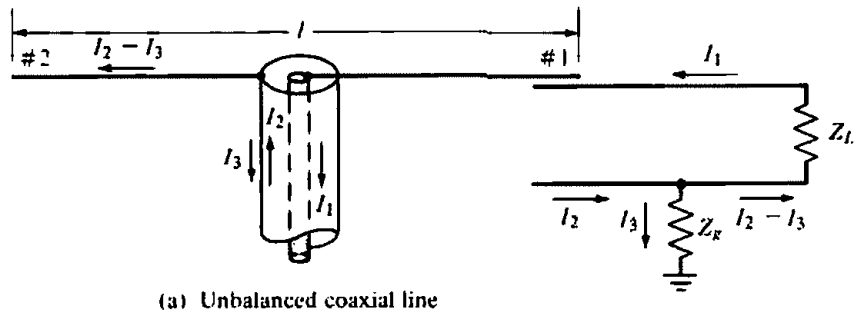

(b) Bazooka balun (1 : 1)

(c) λ/4 coaxial balun (1 : 1)

(d) Coaxial balun (1 : 1)

Figure 9.24 Balun configurations.

(a) $\lambda/2$ coaxial balun (4 : 1 or 1 : 4)

(b) Ferrite core transformer (4 : 1 or 1 : 4)

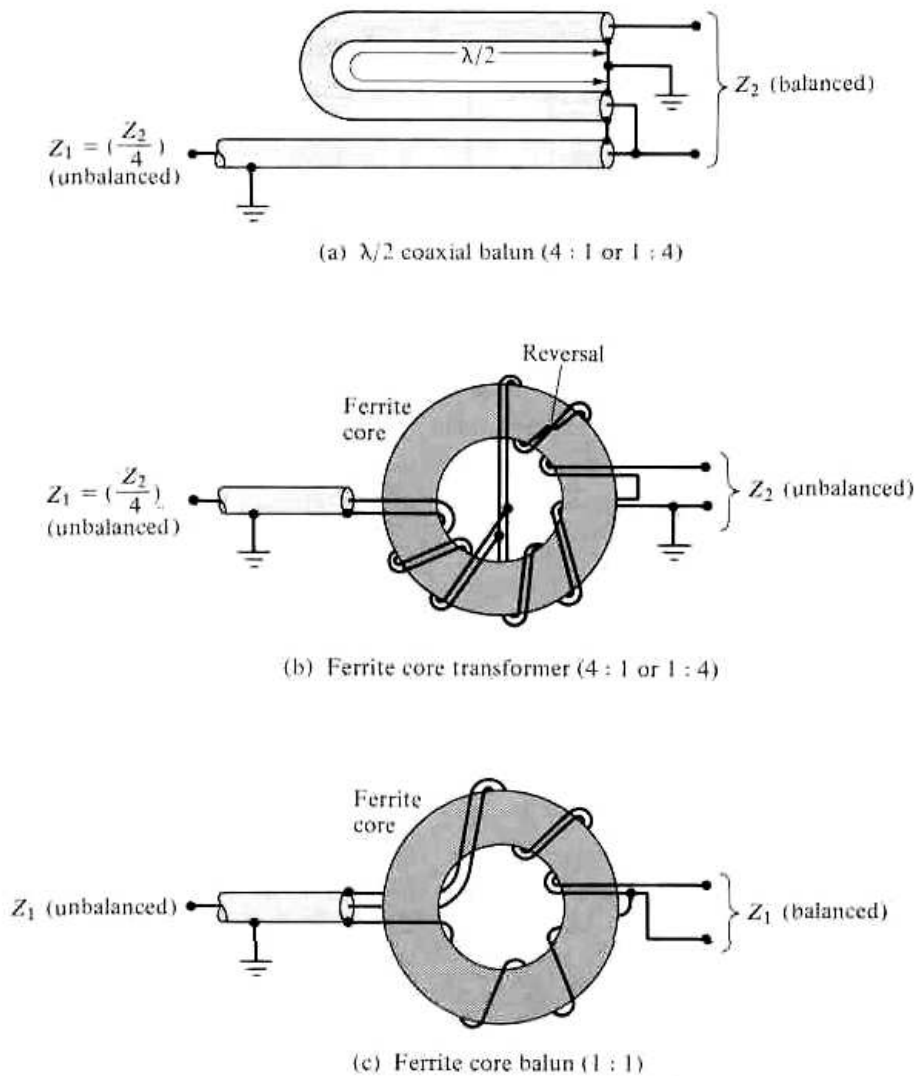(c) Ferrite core balun (1 : 1)

Figure 9.25   Balun and ferrite core transformers.

Another type of a balun is that shown in Figure 9.24(c). It requires that one end of a $\lambda/4$ section of a transmission line be connected to the outside shield of the main coaxial line while the other is connected to the side of the dipole which is attached to the center conductor. This balun is used to cancel the flow of I_3. The operation of it can be explained as follows: In Figure 9.24(a) the voltages between each side of the dipole and the ground are equal in magnitude but 180° out of phase, thus producing a current flow on the outside of the coaxial line. If the two currents I_1 and I_2 are equal in magnitude, I_3 would be zero. Since terminal #2 of the dipole is connected directly to the shield of the coax while terminal #1 is weakly coupled to it, it produces a much larger current I_2. Thus there is relatively little cancellation in the two currents.

The two currents, I_1 and I_2, can be made equal in magnitude if the center conductor of the coax is connected directly to the outer shield. If this connection is made directly at the antenna terminals, the transmission line and the antenna would be short-circuited, thus eliminating any radiation. However, the indirect parallel conductor connection of Figure 9.24(c) provides the desired current cancelation without eliminating the radiation. The current flow on the outer shield of the main line is canceled at the bottom end of the $\lambda/4$ section (where the two join together) by the equal in magnitude, but opposite in phase, current in the $\lambda/4$ section of the auxiliary line. Ideally then there is no current flow in the outer surface of the outer shield of the remaining part

of the main coaxial line. It should be stated that the parallel auxiliary line need not be made λ/4 in length to achieve the balance. It is made λ/4 to prevent the upsetting of the normal operation of the antenna.

A compact construction of the balun in Figure 9.24(c) is that in Figure 9.24(d). The outside metal sleeve is split and a portion of it is removed on opposite sides. The remaining opposite parts of the outer sleeve represent electrically the two shorted λ/4 parallel transmission lines of Figure 9.24(c). All of the baluns shown in Figure 9.24 are narrowband devices.

Devices can be constructed which provide not only balancing but also step-up impedance transformations. One such device is the λ/4 coaxial balun, with a 4:1 impedance transformation, of Figure 9.25(a). The U-shaped section of the coaxial line must be λ/2 long [22].

Because all the baluns-impedance transformers that were discussed so far are narrowband devices, the bandwidth can be increased by employing ferrite cores in their construction [23]. Two such designs, one a 4:1 or 1:4 transformer and the other a 1:1 balun, are shown in Figures 9.25(b) and (c). The ferrite core has a tendency to maintain high impedance levels over a wide frequency range [24]. A good design and construction can provide bandwidths of 8 or even 10 to 1. Coil coaxial baluns, constructed by coiling the coaxial line itself to form a balun [24], can provide bandwidths of 2 or 3 to 1.

References

1. M. Abraham. "Die electrischen Schwingungen um einen stabformingen Leiter, behandelt nach der Maxwelleschen Theorie." *Ann. Physik*, 66, pp. 435–472, 1898.
2. S. A. Schelkunoff. *Electromagnetic Waves*, Van Nostrand, New York, 1943, Chapter 11.
3. E. Hallén, "Theoretical Investigations into the Transmitting and Receiving Qualities of Antennae," *Nova Acta Regiae Soc. Sci. Upsaliensis*, Ser. IV, 11, No. 4, pp. 1–44, 1938.
4. R. C. Johnson and H. Jasik (eds.), *Antenna Engineering Handbook*, McGraw-Hill, New York, 1984, Chapter 4.
5. G. H. Brown and O. M. Woodward, Jr., "Experimentally Determined Radiation Characteristics of Conical and Triangular Antennas," *RCA Rev.*, Vol. 13, No. 4, p. 425, December 1952.
6. C. H. Papas and R. King, "Radiation from Wide-Angle Conical Antennas Fed by a Coaxial Line," *Proc. IRE*, Vol. 39, p. 1269, November 1949.
7. C. E. Smith, C. M. Butler, and K. R. Umashankar, "Characteristics of a Wire Biconical Antenna," *Microwave Journal*, pp. 37–40, September 1979.
8. G. H. Brown and O. M. Woodward, Jr., "Experimentally Determined Impedance Characteristics of Cylindrical Antennas," *Proc. IRE*, Vol. 33, pp. 257–262, 1945.
9. J. D. Kraus, *Antennas*, McGraw-Hill, New York, 1950, pp. 276–278.
10. J. H. Richmond and E. H. Newman, "Dielectric Coated Wire Antennas," *Radio Science*, Vol. 11, No. 1, pp. 13–20, January 1976.
11. J. Y. P. Lee and K. G. Balmain, "Wire Antennas Coated with Magnetically and Electrically Lossy Material," *Radio Science*, Vol. 14, No. 3, pp. 437–445, May-June 1979.
12. G. A. Thiele, E. P. Ekelman, Jr., and L. W. Henderson, "On the Accuracy of the Transmission Line Model for Folded Dipole," *IEEE Trans. Antennas Propagat.*, Vol. AP-28, No. 5, pp. 700–703, September 1980.
13. R. W. Lampe, "Design Formulas for an Asymmetric Coplanar Strip Folded Dipole," *IEEE Trans. Antennas Propagat.*, Vol. AP-33, No. 9, pp. 1028–1031, September 1985.
14. A. G. Kandoian, "Three New Antenna Types and Their Applications," *Proc. IRE*, Vol. 34, pp. 70W–75W, February 1946.

15. R. W. King and T. T. Wu, "The Cylindrical Antenna with Arbitrary Driving Point," *IEEE Trans. Antennas Propagat.*, Vol. AP-13, No. 5, pp. 710–718, September 1965.

16. R. W. P. King, "Asymmetric Driven Antennas and the Sleeve Dipole," *Proc. IRE*, Vol. 38, pp. 1154–1164, October 1950.

17. R. E. Collin, *Foundations for Microwave Engineering*, McGraw-Hill, New York, 1992, Chapter 5, pp. 303–386.

18. S. Y. Liao, *Microwave Devices and Circuits*, Prentice-Hall, Englewood Cliffs, New Jersey, 1980, pp. 418–422.

19. D. J. Healey, III, "An Examination of the Gamma Match," *QST*, pp. 11–15, April 1969.

20. *The ARRL Antenna Book*, American Radio Relay League, Inc., Newington, Conn., 1974, pp. 118–121.

21. H. T. Tolles, "How To Design Gamma-Matching Networks," *Ham Radio*, pp. 46–55, May 1973.

22. O. M. Woodward, Jr., "Balance Measurements on Balun Transformers," *Electronics*, Vol. 26, No. 9, September 1953, pp. 188–191.

23. C. L. Ruthroff, "Some Broad-Band Transformers," *Proc. IRE*, Vol. 47, August 1959, pp. 1337–1342.

24. W. L. Weeks, *Antenna Engineering*, McGraw-Hill, New York, 1968, pp. 161–180.

PROBLEMS

9.1. A 300-ohm "twin-lead" transmission line is attached to a biconical antenna.

   (a) Determine the cone angle that will match the line to an infinite length biconical antenna.

   (b) For the cone angle of part (a), determine the two smallest cone lengths that will resonate the antenna.

   (c) For the cone angle and cone lengths from part (b), what is the input VSWR?

9.2. Determine the first two resonant lengths, and the corresponding diameters and input resistances, for dipoles with $l/d = 25, 50,$ and 10^4 using

   (a) the data in Figures 9.8(a) and 9.8(b)

   (b) Table 9.1

9.3. Design a resonant cylindrical stub monopole of length l, diameter d, and l/d of 50. Find the length (in λ), diameter (in λ), and the input resistance (in ohms) at the first four resonances.

9.4. A linear dipole of $l/d = 25, 50,$ and 10^4 is attached to a 50-ohm line. Determine the VSWR of each l/d when

   (a) $l = \lambda/2$

   (b) $l = \lambda$

   (c) $l = 3\lambda/2$

9.5. Find the equivalent circular radius a_e for a

   (a) very thin flat plate of width $\lambda/10$

   (b) square wire with sides of $\lambda/10$

   (c) rectangular wire with sides of $\lambda/10$ and $\lambda/100$

   (d) elliptical wire with major and minor axes of $\lambda/10$ and $\lambda/20$

   (e) twin-lead transmission line with wire radii of 1.466×10^{-2} cm and separation of 0.8 cm

9.6. Compute the characteristic impedance of a two-wire transmission line with wire diameter of $d = 10^{-3}\lambda$ and center-to-center spacings of

   (a) $6.13 \times 10^{-3}\lambda$

   (b) $2.13 \times 10^{-2}\lambda$

   (c) $7.42 \times 10^{-2}\lambda$

9.7. Verify (9-47) from the expressions listed in Table 9.3.

9.8. To increase its bandwidth, a $\lambda/4$ monopole antenna operating at 1 GHz is made of two side-by-side copper wires ($\sigma = 5.7 \times 10^7$ S/m) of circular cross section. The wires at

each end of the arm are connected (shorted) electrically together. The radius of each wire is $\lambda/200$ and the separation between them is $\lambda/50$.

(a) What is the effective radius (in meters) of the two wires? Compare with the physical radius of each wire (in meters).

(b) What is the high-frequency loss resistance of each wire? What is the total loss resistance of the two together in a side-by-side shorted at the ends arrangement? What is the loss resistnce based on the effective radius?

(c) What is the radiation efficiency of one wire by itself? Compare with that of the two together in a side-by-side arrangement. What is the radiation efficiency based on the loss resistance of the effective radius?

9.9. Show that the input impedance of a two-element folded dipole of $l = \lambda/2$ is four times greater than that of an isolated element of the same length.

9.10. Design a two-element folded dipole with wire diameter of $10^{-3}\lambda$ and center-to-center spacing of $6.13 \times 10^{-3}\lambda$.

(a) Determine its shortest length for resonance.

(b) Compute the VSWR at the first resonance when it is attached to a 300-ohm line.

9.11. A two-element folded dipole of identical wires has an $l/d = 500$ and a center-to-center spacing of $6.13 \times 10^{-3}\lambda$ between the wires. Compute the

(a) approximate length of a single wire at its first resonance

(b) diameter of the wire at the first resonance

(c) characteristic impedance of the folded dipole transmission line

(d) input impedance of the transmission line mode model

(e) input impedance of the folded dipole using as the radius of the antenna mode (1) the radius of the wire a, (2) the equivalent radius a_e of the wires, (3) half of the center-to-center spacing ($s/2$). Compare the results.

9.12. The input impedance of a 0.47λ folded dipole operating at 10 MHz is

$$Z_{in} = 306 + j75.3$$
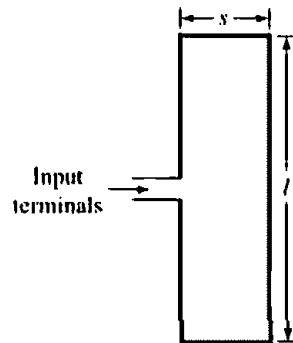
To resonate the element, it is proposed to place a lumped element in shunt (parallel) at the input terminals where the impedance is measured.

(a) What kind of an element (capacitor or inductor) should be used to accomplish the requirement?

(b) What is the value of the element (in farads or henries)?

(c) What is the new value of the input impedance?

(d) What is the VSWR when the resonant antenna is connected to a 300-ohm line?

9.13. A half-wavelength, two-element symmetrical folded dipole is connected to a 300-ohm "twin-lead" transmission line. In order for the input impedance of the dipole to be real, an energy storage lumped element is placed across its input terminals. Determine, assuming $f = 100$ MHz, the

(a) capacitance or inductance of the element that must be placed across the terminals.

(b) VSWR at the terminals of the transmission line taking into account the dipole and the energy storage element.

9.14. A half-wavelength, two-element symmetrical folded dipole whose each wire has a radius of $10^{-3}\lambda$ is connected to a 300-ohm "twin-lead" transmission line. The center-to-center spacing of the two wires is $4 \times 10^{-3}\lambda$. In order for the input impedance of the dipole to be real, determine, assuming $f = 100$ MHz, the

(a) total capacitance C that must be placed in series at the input terminals.

(b) capacitance C_L (two of them) that must be placed in series at each of the input terminals of the dipole in order to keep the antenna symmetrical.

(c) VSWR at the terminals of the transmission line connected to the dipole through the two capacitances.

9.15. An $l = 0.47\lambda$ folded dipole, whose wire radius is $5 \times 10^{-3}\lambda$, is fed by a "twin lead" transmission line with a 300-ohm characteristic impedance. The center-to-center spacing of the two side-by-side wires of the dipole is $s = 0.025\lambda$. The dipole is operating at $f = 10$ MHz. The input impedance of the "regular" dipole of $l = 0.47\lambda$ is $Z_d = 79 + j13$.

(a) Determine the
    i. Input impedance of the folded dipole.
    ii. Amplification factors of the real and imaginary parts of the input impedance of the folded dipole, compared to the corresponding values of the regular dipole.
    iii. Input reflection coefficient.
    iv. Input VSWR.

(b) To resonate the folded dipole and keep the system balanced, two capacitors (each C) are connected each symmetrically in series at the input terminals of the folded dipole.
    i. What should C be to resonate the dipole?
    ii. What is the new reflection coefficient at the input terminals of the "twin lead" line?
    iii. What is the new VSWR?

9.16. A $\lambda/2$ dipole is fed asymmetrically at a distance of $\lambda/8$ from one of its ends. Determine its input impedance using (9-32). Compare its value with that obtained using the impedance transfer method of Section 4.5.5.

9.17. Repeat the design of Example 9.1 using a Tschebyscheff transformer.

9.18. Repeat the design of Example 9.1 for a three-section
(a) binomial transformer
(b) Tschebyscheff transformer

9.19. A self-resonant (first resonance) half-wavelength dipole of radius $a = 10^{-3}\lambda$ is connected to a 300-ohm "twin-lead" line through a three-section binomial impedance transformer. Determine the impedances of the three-section binomial transformer required to match the resonant dipole to the "twin-lead" line.

9.20. Consider a center-fed thin-wire dipole with wire radius $a = 0.005\lambda$.

(a) Determine the resonant length l (in wavelengths) and corresponding input resistance R_{in} of the antenna using assumed sinusoidal current distribution.

(b) Design a two-section Tschebyscheff quarter-wavelength transformer to match the antenna to a 75-ohm transmission line. Design the transformer to achieve an equal ripple response to R_{in} over a fractional bandwidth of 0.25.

(c) Compare the performance of the matching network in part (b) to an ideal transformer by plotting the input reflection coefficient magnitude versus normalized frequency for $0 \le f/f_0 \le 2$ for both cases.

9.21. The free-space impedance at the center point of the driven element of a 15-MHz Yagi-Uda array is $25 - j25$. Assuming the diameters of the wires of a T-match are $1.9 \times 10^{-3}\lambda(3.8 \text{ cm})$ and $6.35 \times 10^{-4}\lambda(1.27 \text{ cm})$, the center-to-center spacing between the wires is $7.62 \times 10^{-3}\lambda(15.24 \text{ cm})$, and the length $l'/2$ of each T-match rod is 0.0285λ (57 cm), find the

(a) input impedance of the T-match
(b) input capacitance C_{in} that will resonate the antenna
(c) capacitance C that must be used in each leg to resonate the antenna

9.22.   The input impedance of a 145.4 MHz Yagi-Uda antenna is $14 + j3$. Design a gamma match using diameters of 0.9525 cm (for the antenna) and 0.2052 cm (for the rod), and center-to-center spacing between the wires of 1.5316 cm. The match is for a 50-ohm input coaxial line. Find the shortest gamma rod length and the required capacitance. First, do the problem analytically. The design must be such that the real part of the designed input impedance is *within 1 ohm* of the required 50 ohms. Second, check your answers with the Smith chart.

9.23.   Repeat Problem 9.22 for an input impedance of $14 - j3$.

9.24.   A $\lambda/4$ monopole is mounted on a ground plane and has an input impedance of $34 + j17$ at $f = 145.4$ MHz. Design a gamma match to match the monopole to a 50-ohm coaxial line. The wire diameters are identical (0.9525 cm) and the center-to-center spacing is 3.1496 cm. Find the required capacitance and the shortest gamma rod length. First, do the problem analytically. The design must be such that the real part of the designed input impedance is *within 1 ohm* of the required 50 ohms. Second, check your answers with the Smith chart.

9.25.   Using a gamma match, a $\lambda/2$ dipole is connected to an amateur 425 MHz radio receiver using a 78-ohm coaxial line. The length of the gamma match is $\lambda/4$ and its wire radius is identical to that of the dipole.

   (a) What is the input impedance of the antenna-gamma match arrangement at the input terminals in the absence of a matching capacitor?
   (b) To resonate the antenna, a capacitor is placed in series to the arm that is connected to the center conductor of the coaxial line. What is the value of the capacitor?
   (c) When the resonant antenna is connected to a 78-ohm coaxial line, what is the magnitude of the reflection coefficient? What is the VSWR?

9.26.   A 300 MHz resonant $\lambda/2$ dipole with an input impedance of 67 ohms is connected to a coaxial line through a gamma match. The radii of the wires for the dipole and gamma match, and the spacing between them, are such that the turns ratio of the transformer is 3:1. The characteristic impedance of the transmission line that the dipole and gamma match part form is 250 ohms. The overall length of the gamma match is 0.1λ.

   (a) What is the total input impedance at the input terminals of the gamma match?
   (b) What value of capacitor placed in series shall be selected so that the new input impedance is real (resonate the load)?

9.27.   A T-match is connected to the antennas of Problems 9.22 and 9.23. Assuming that the wire diameters and lengths for each leg of the T-match are those derived for each gamma match, find the

   (a) input impedance of the T-match
   (b) capacitance C that must be connected in each leg to make the antenna system resonant

9.28.   Repeat Problem 9.27 but select the lengths $l'/2$ of the T-match rods so that the input resistance is 300 ohms. Use diameters of 0.1026 cm (for the rod), 0.9525 cm (for the antenna), and center-to-center spacing of 0.7658 cm. This connection is ideal for use with a 300-ohm "twin-lead" line.